The Abdus Salam
International Centre for Theoretical Physics

United Nations
Educational, Scientific and
Cultural Organization

IAEA
International Atomic Energy Agency

1856-32

2007 Summer College on Plasma Physics

30 July - 24 August, 2007

Beam-plasma interaction in the solar wind and electron foreshock region

V. Krasnosselskikh
LPCE/CNRS
University of Orleans
Orleans, France

V. Lobzin, T. Dudok de Wit, J. Soucek, K. Musatenko, I. Cairns & J. Pickett
LPCE/CNRS
University of Orleans
Orleans, France

Beam-plasma interaction in the solar wind and electron foreshock region

Vladimir Krasnoselskikh

LPCE/CNRS-University of Orleans

with co-authors

V. Lobzin, T. Dudok de Wit, J. Soucek, K. Musatenko, I. Cairns & J. Pickett

Beam-plasma interaction

Conventional approach:

Linear instability

Growth rate and the stage of exponential growth

$$E \approx E_0 \exp(-i\omega t + \gamma t + i\vec{k}\vec{r})$$

$$\gamma = -\operatorname{Im}\varepsilon / (\partial \operatorname{Re}\varepsilon / \partial\omega)$$

Saturation of the instability :

Wave-particle interaction or / and nonlinear process in game

Beam plasma interaction in homogeneous plasma (courtesy of E. Marsch)

Gentle beam instability I

Electromagnetic waves can penetrate a plasma from outside, whereas electrostatic waves must be excited internally. The simplest kinetic instability is that of an electron beam propagating on a uniform background: ***gentle beam*** or ***bump-on-tail*** configuration:

$$\omega_l = \pm\omega_{pe}\left(1+\frac{3}{2}k^2\lambda_D^2\right)+i\gamma_l(k)$$

Few fast electrons at speed $v_b >> v_{th0}$, but with $n_b << n_0$, can excite Langmuir waves.

$$\gamma_l = \omega_l \frac{\pi\omega_{pe}^2}{2n_0k^2}\frac{\partial f_{0e}(v)}{\partial v}\Big|_{v=\omega/k}$$

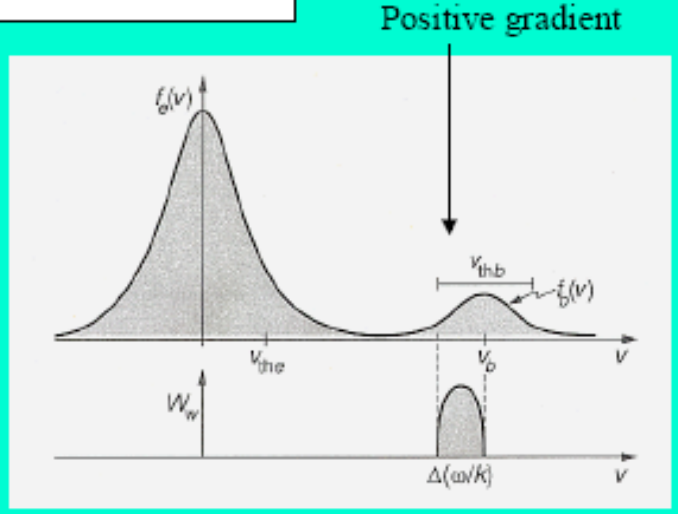

Beam plasma interaction in electron foreshock region and in solar wind (courtesy of E. Marsch)

Gentle beam instability II

To calculate the growth rate (left as an exercise) of the ***gentle beam*** instability, we consider the sum of two Maxwellians:

$$f_{0e}(v) = f_0(v) + f_b(v - v_b)$$

The maximum growth rate is obtained for a cool, fast and dense beam.

The condition for growth of Langmuir waves is that the beam velocity exceeds a threshold, $v_b > \sqrt{3}\, v_{th0}$, in order to overcome the Landau damping of the main part of the VDF. Electron beams occur in front of the ***bow shock*** and often in the solar corona during solar ***flares***.

$$\gamma_{gb,max} = \left(\frac{\pi}{2e}\right)^{1/2} \frac{n_b}{n_0} \left(\frac{v_b}{v_{thb}}\right)^2 \omega_l$$

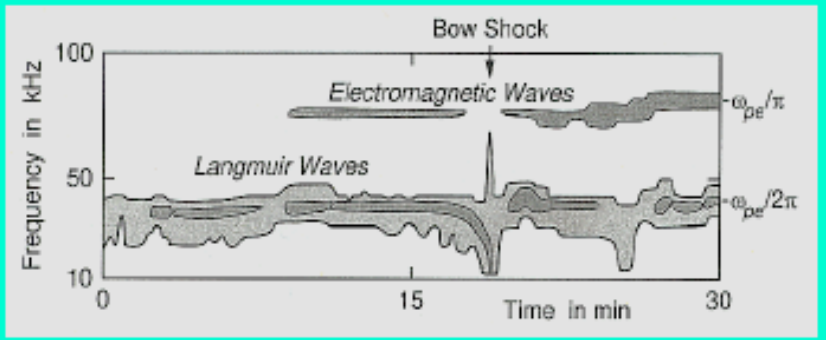

Energetic electrons and type III bursts

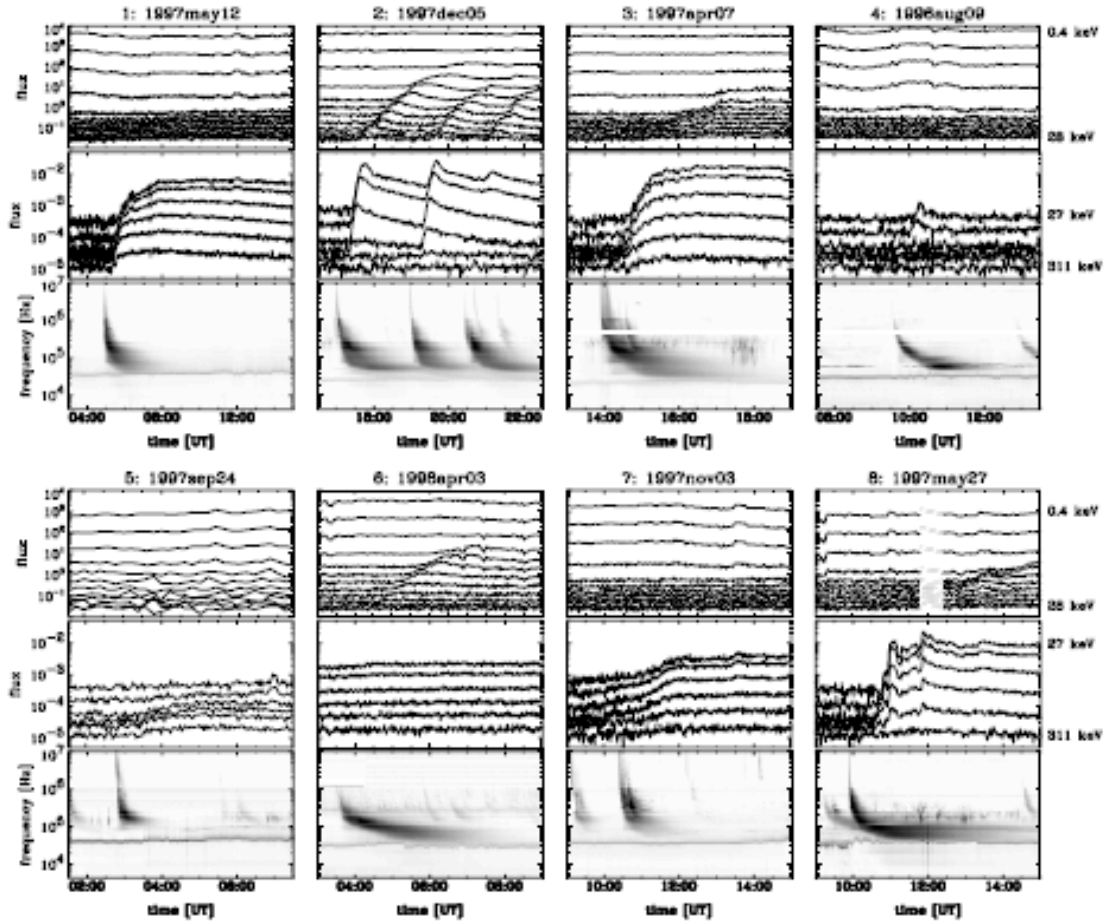

FIG. 1.—Overview plots of eight impulsive electron events. For each event, the two top panels show the observed electron flux at 1 AU: the top panels for the energy range of 0.4 (*top curve*) to 27.7 keV (*bottom curve*) and the middle panels for 26.8 (*top curve*) to 31 keV (*bottom curve*). In the bottom panels the radio spectrograms observed by *Wind* Waves instrument (Bougeret et al. 1995) are displayed. The dark areas are enhanced emission. For an easier comparison between these events, the time periods shown are equal in length (6 hr) and the flux and frequency axes are the same for all events. Starting at the top right, the events can be described as (1) event only at high energies; (2) multiple events down to energies around 1 keV; (3) event similar to event 1, with an additional weak enhancement at low energies; (4) weak event observed only at two energies; (5) very weak event at high energies; (6) event only at low energies; (7) complex event; and (8) solar event with no clear velocity dispersion.

Type II and type III radiobursts

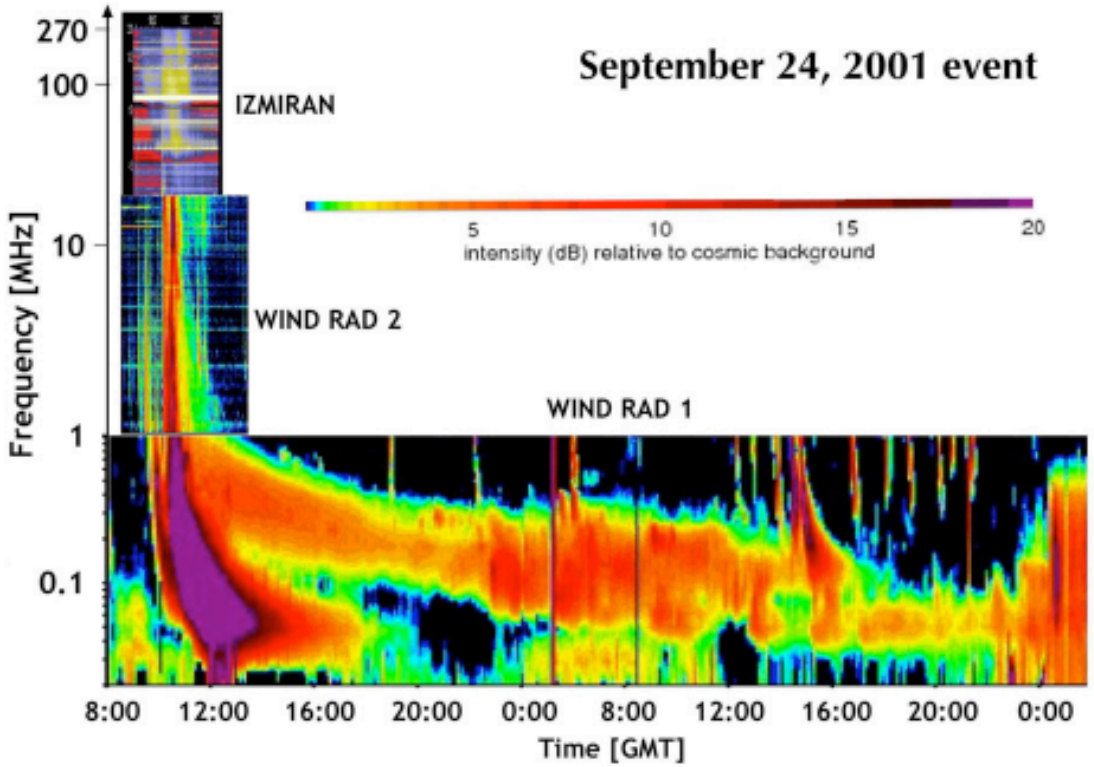

Figure 1. Combined measurements of type III / type II bursts observed onboard Wind satellite (RAD 1 and RAD 2 instruments) and by IZMIRAN radio-telescope

Type III EM waves and Langmuir waves (courtesy of E. Marsch)

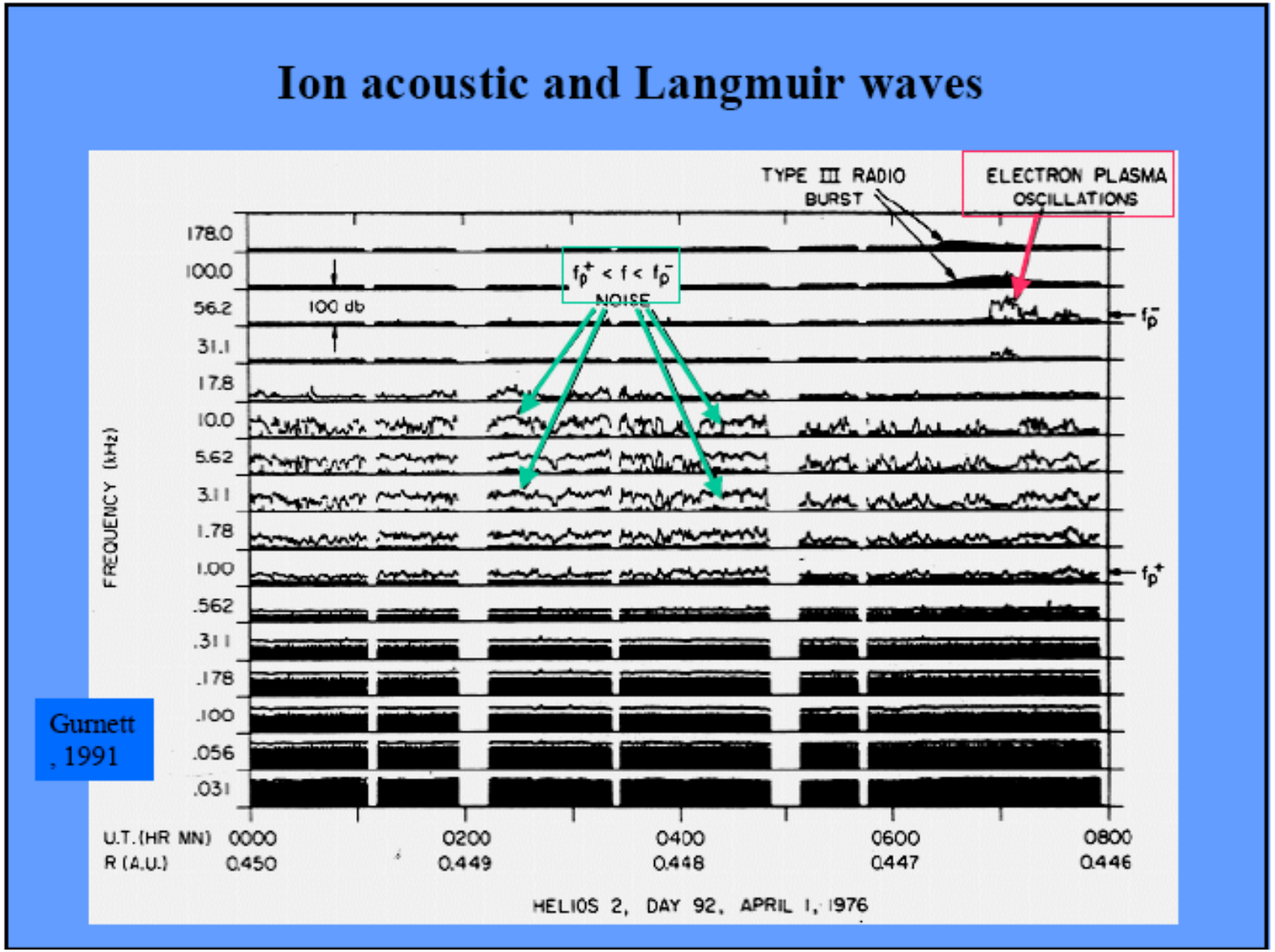

Bump on tail feature of electron distribution

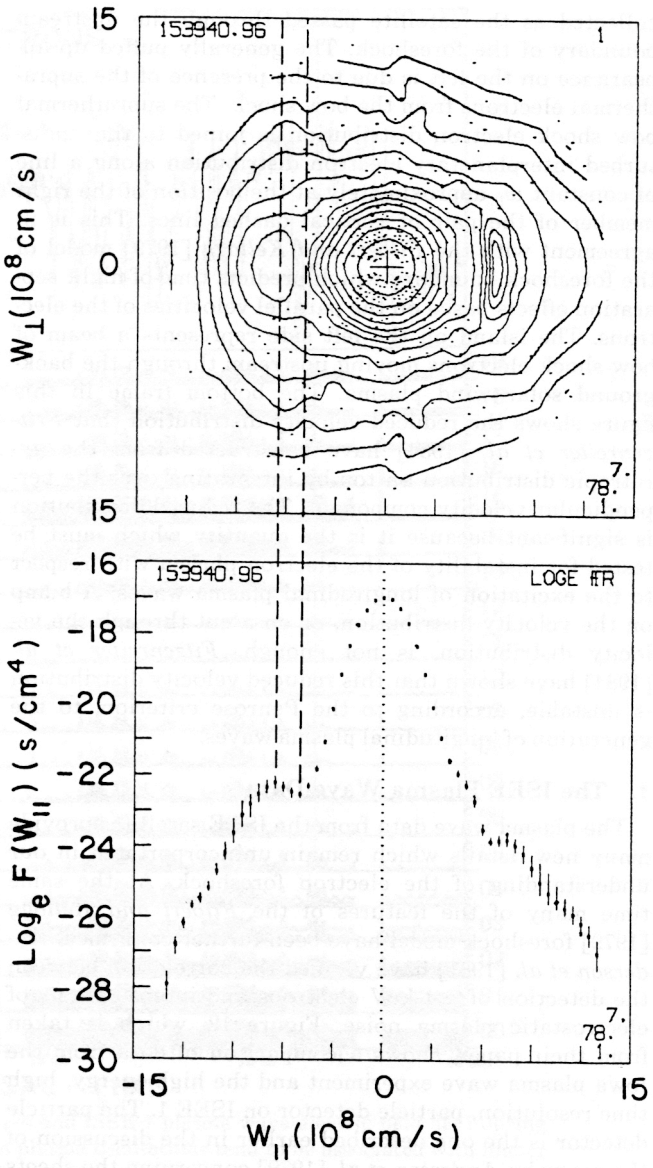

Contour map of the surface $f(W_{||}, W_\perp)$ obtained from a three dimensional measurements of the electron velocity distribution at the electron foreshock boundary on November 6 1977 at 15:39:41 – 44 UT. The reduced distribution $f(W_{||})$ (bottom) shows a bump on the tail at

$W_{||} = -7*10^8$ cm/sec and the vertical dached lines outline the elemental strip of parallel velocity space producing the positive slope [from Fitzenreiter et al., 1984].

Electron flux events and waves

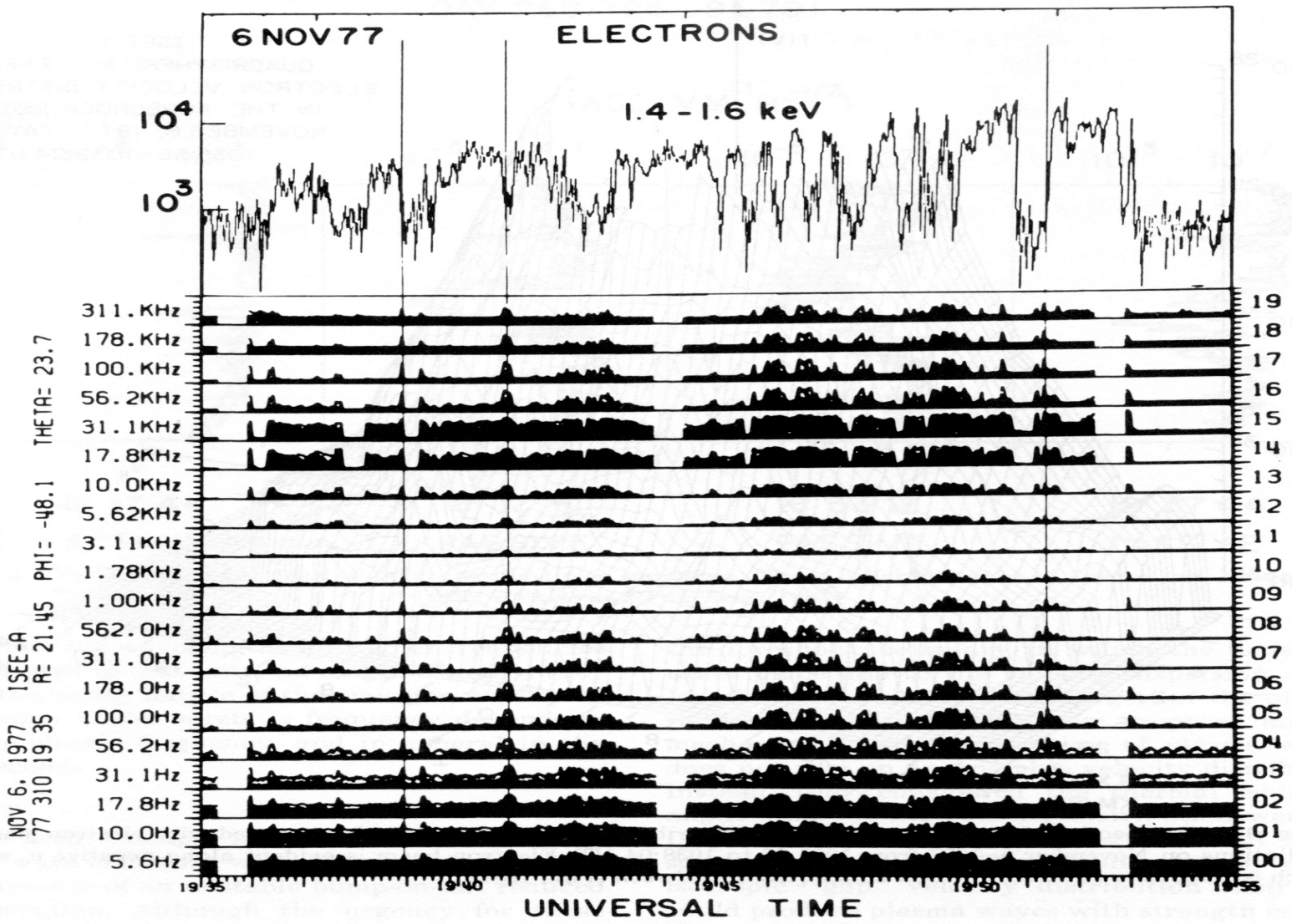

Fig. 12. An expanded display of energetic electron fluxes and ISEE 1 plasma wave electric field data during an electron flux event. Note how the more intense electron plasma oscillations tend to be associated with higher fluxes of low-energy electrons. The electron plasma oscillations and low-frequency electrostatic waves are also enhanced at gradients in the energetic electron density [from *Anderson et al.*, 1981].

Why beams are around electron foreshock ? (courtesy of Gedalin)

Electron and ion foreshock geometries

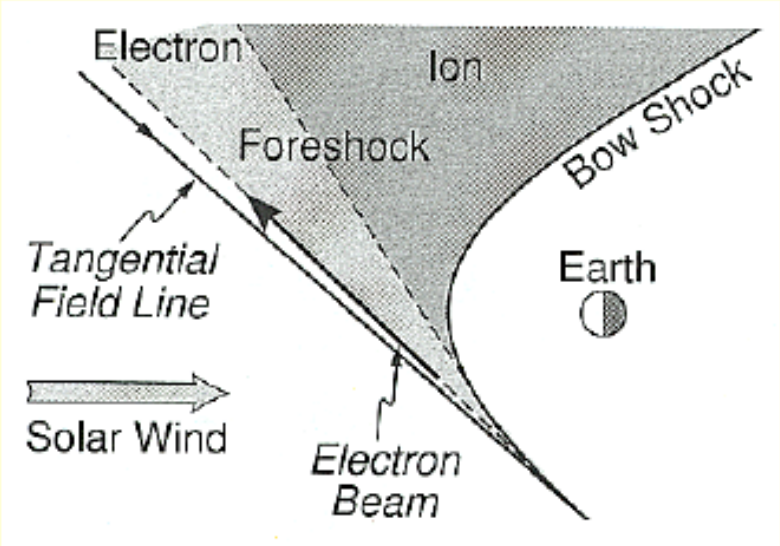

In the de Hoffman-Teller frame one moves parallel to the schock surface with a velocity v_{HT}, which transforms the upstream solar wind inflow velocity into a velocity that is entirely parallel to the upstream magnetic field. This velocity can be expressed by the shock normal unit vector, **n.**

$$\mathbf{v}_{sw} = \mathbf{v}_{HT} + \mathbf{v}_{sw\|}$$

$$\mathbf{v}_{HT} = \hat{\mathbf{n}} \times (\mathbf{v}_{sw} \times \mathbf{B}_{sw}) / \hat{\mathbf{n}} \cdot \mathbf{B}_{sw}$$

Different possible variants

- QL saturation and plateau type particle distribution formation (Vedenov, Velikhov & Sagdeev, 1962, Drummond & Pines, 1962, Romanov & Filippov, 1961)

  Physical picture: diffusion of particles in the field of many waves

  Finite amplitude sinusoidal electrostatic wave can trap the particle

Trapping of particles (courtesy of E. Marsch)

Particle trapping in waves

One of the simplest nonlinear effects is ***trapping of particles*** in large-amplitude waves, in which the wave potential exceeds the particle kinetic energy. Trapping is largest for resonant particles, which are moving at the wave phase speed and see a nearly stationary electrostatic potential:

$$\phi(x,t) = \phi_0 \cos(kx - \omega t) = \phi_0 \cos(kx')$$

Here the coordinates were transformed into the wave frame by

$$x' = x - (\omega/k)t$$

The particle speed is also transformed by

$$v' = v - \omega/k$$

The particle's total energy in the wave frame is

$$W_e = \frac{1}{2}mv'^2 - e\phi_0 \cos(kx')$$

Trapping of particles (courtesy of E. Marsch)

Trajectories of trapped particles

When considering electron motion in ***two-dimenensional phase space*** (x', v'), particles move along ***lines of constant energy*** W_e, as is shown below.

There appear to be two types of trajectories:

- ***closed*** **trajectories** with $W_e < 0$, ***trapped*** particles
- ***open*** **trajectories** with $W_e > 0$, ***untrapped*** particles

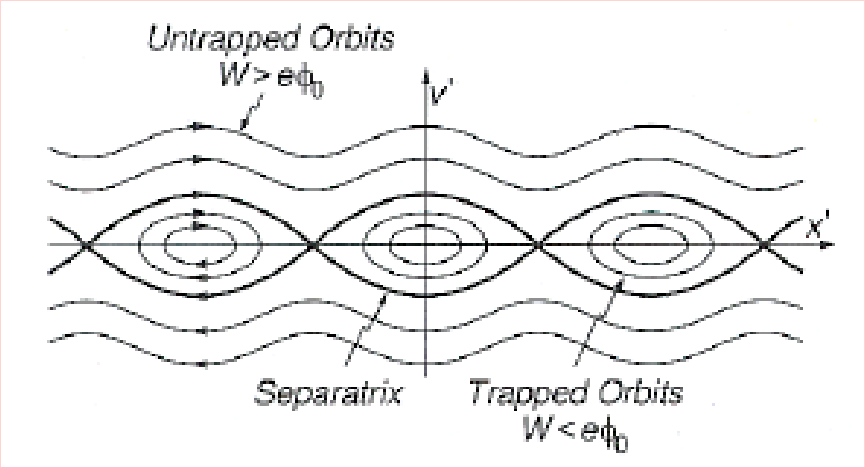

The trapped particles bounce back and force between the potential walls and oscillate periodically (expand the cosine potential) with the trapping frequency:

The larger the amplitude, ϕ_0, the faster is the oscillation.

$$\omega_b = |e\phi_0 k^2/m|^{1/2}$$

Quasilinear description (courtesy of Marsch)

Perturbation theory

Nonlinear interaction can lead to stationary states consisting of large-amplitude waves and related particle distributions of trapped and free populations. It is difficult to find these states, and often ***perturbation*** expansions are used, leading to what is called ***weak plasma turbulence*** theory. Starting point is the coupled system of **Maxwell's** (which we do not quote here) and **Vlasov's** equations, e.g. for the *s*-component of the plasma.

$$\frac{\partial f_s}{\partial t} + \mathbf{v} \cdot \nabla f_s + \frac{q_s}{m_s} (\mathbf{E} + \mathbf{v} \times \mathbf{B}) \cdot \frac{\partial f_s}{\partial \mathbf{v}} = 0$$

We split the fields and velocity distributions into average slowly varying parts, f_{s0}, $\mathbf{E}_0$, and $\mathbf{B}_0$, and oscillating parts, δf_s, $\delta\mathbf{E}$ and $\delta\mathbf{B}$, and assume that the long-time and large-volume averages over fluctuations vanish, i.e.

$$\langle \delta f_s \rangle = \langle \delta \mathbf{E} \rangle = \langle \delta \mathbf{B} \rangle = 0$$

Averaging the resulting Vlasov equation gives the evolution for f_{s0}. No assumptions were yet made about the size of the fluctuations, but usually they are assumed to be much smaller than the background.

Quasilinear equation (courtesy of E. Marsch)

Quasilinear theory

The **Vlasov** equation for the slowly-varying ensemble averaged VDF of species *s* reads:

$$\frac{\partial f_{s0}}{\partial t} + \mathbf{v}\cdot\nabla f_{s0} + \frac{q_s}{m_s}(\mathbf{v}\times\mathbf{B})\cdot\frac{\partial f_{s0}}{\partial \mathbf{v}} = -\frac{q_s}{m_s}\left\langle(\delta\mathbf{E}+\mathbf{v}\times\delta\mathbf{B})\cdot\frac{\partial \delta f_s}{\partial \mathbf{v}}\right\rangle$$

The second-order interactions between the fluctuations, δf_s, $\delta\mathbf{E}$ and $\delta\mathbf{B}$, appear on the right-hand side. If they are small we speak of ***quasilinear theory***. This fundamental equation describes the nonlinear dynamics of the plasma. ***It results from the scattering of particle motion in the short-wavelength, high-frequency field fluctuations.***

Formally the perturbation series can, with the smallness parameter λ, be written as:

$$\begin{aligned} f_s &= f_{s0} + \lambda\delta f_{s1} + \lambda^2\delta f_{s2} + \ldots \\ \delta\mathbf{E} &= \lambda\delta\mathbf{E}_1 + \lambda^2\delta\mathbf{E}_2 + \ldots \end{aligned}$$

Application to beam-plasma instability (courtesy of E. Marsch)

Weak gentle-beam turbulence I

The perturbation series is expected to converge rapidly, if λ is small. Assume

$$\lambda = \frac{\langle \epsilon_0 |\delta \mathbf{E}(\mathbf{x},t)|^2 \rangle}{2\langle n \rangle k_B \langle T \rangle} \ll 1$$

Assume a gentle source of ***free energy*** in the form of a ***weak beam*** of electrons crossing the plasma and consider the associated excitation of Langmuir waves. Remember that the ***linear complex frequency*** is:

$$\omega(k) = \omega_{pe}\left(1 + \frac{3}{2}k^2\lambda_D^2\right)$$

$$\gamma(k,t) = \omega(k)\frac{\pi\omega_{pe}^2}{2k^2}\frac{\partial f_{0b}(v,t)}{\partial v}\Big|_{v=\omega/k}$$

Consequently, the electric field evolves in time according to:

$$\delta E(k,t) = \delta E(k,0)\exp\left\{-\int_0^t [i\omega(k) - \gamma(k,\tau)]\,d\tau\right\}$$

QL approximation (courtesy of E. Marsch)

Weak gentle-beam turbulence II

Consequently, the average particle VDF will also evolve in time according to:

$$\frac{\partial f_{0b}(v,t)}{\partial t} = \frac{e}{m_e}\left\langle \delta E \frac{\partial \delta f}{\partial v} \right\rangle$$

This quadratic correlation term can be calculated by help of Fourier transformation of the Vlasov equation for the fluctuations, yielding:

$$\delta f(k) = i\frac{e}{m_e}\frac{\delta E(k)}{\omega - kv}\frac{\partial f_{0b}(v,t)}{\partial v}$$

Inserting the first in the second gives a second-order term, $\delta E(\mathbf{k}, \omega)\,\delta E(-\mathbf{k}, -\omega)$, which gives the ***wave power spectrum***. Hence we arrive at the diffusion equation for the beam distribution, with the general diffusion coefficient:

$$D(v,t) = Re\left\{\frac{ie^2}{m_e^2}\sum_k \frac{|\delta E(k)|^2}{kv - \omega(k) + i\gamma(k,t)} \exp\left[2\int_0^t \gamma(k,\tau)d\tau\right]\right\}$$

Diffusion equation in the velocity space (courtesy of E. Marsch)

Diffusion equation

Through diffusion of particles in the wave field, the average VDF will slowly evolve in time according to:

$$\frac{\partial f_{0b}(v,t)}{\partial t} = \frac{\partial}{\partial v}\left[D(v,t)\frac{\partial f_{0b}(v,t)}{\partial v}\right]$$

This is a special case of a ***Fokker-Planck equation***, typically arising in quasilinear theory. The beam distribution will spread with time in velocity space under the action of the unstable Langmuir fluctuations. The resonant denominator may be replaced by a delta function giving:

$$D(v,t) = \frac{\pi e^2}{m_e^2}\int W_w(k,t)\delta(\omega - kv)dk$$

By differentiation of the wave electric field, $\delta E(x, t)$, we obtain the evolution equation of the associated spectral density as follows:

$$\frac{\partial W_w(k,t)}{\partial t} = 2\gamma(k,t)W_w(k,t)$$

This completes the ***quasilinear equations*** of beam-excited Langmuir waves.

Plateau as a result of QL diffusion (courtesy of E. Marsch)

Plateau formation

The validity of the quasilinear equations requires that

$$\gamma/\omega \gg W_w/n_0 k_B T_e$$

Fortunately, the equations allow some clear insights into the underlying physics.
Inspection of the diffusion equation shows, that a steady final VDF occurs if

$$D(v,\infty)\frac{\partial f_{0b}(v,\infty)}{\partial v} = 0$$

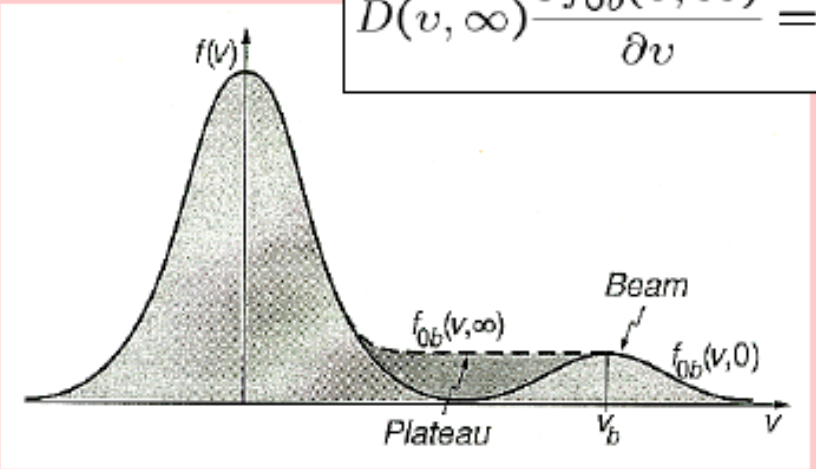

This implies that the gradient flattens and disappears, since the spectrum is positive definite, and the diffusion coefficient is only zero if the entire spectrum vanishes.

As a final result, a plateau will form by diffusion in velocity space.

Some estimates

$$W = \varepsilon_0 E^2 = \frac{1}{2} m \int_0^v v^2 (f_0^0 - f_0^\infty) dv \sim n_b m V_b \Delta V_b$$

$$\frac{\partial f}{\partial t} = \frac{\partial}{\partial v} D \frac{\partial f}{\partial v}$$

$$D = \frac{\omega_p^2}{m n_0 v} W$$

$$\tau \simeq \frac{\Delta V_b^2}{D}$$

$$L \sim V_b \tau$$

Another possibilities for intense beams

- Weak turbulence
- a) decay instability
- L → L + S
- b) induced scattering on ions
- L → L + i

- Strong turbulence: formation of solitons and collapse

What is wrong with our models ?

Compressive fluctuations in the solar wind

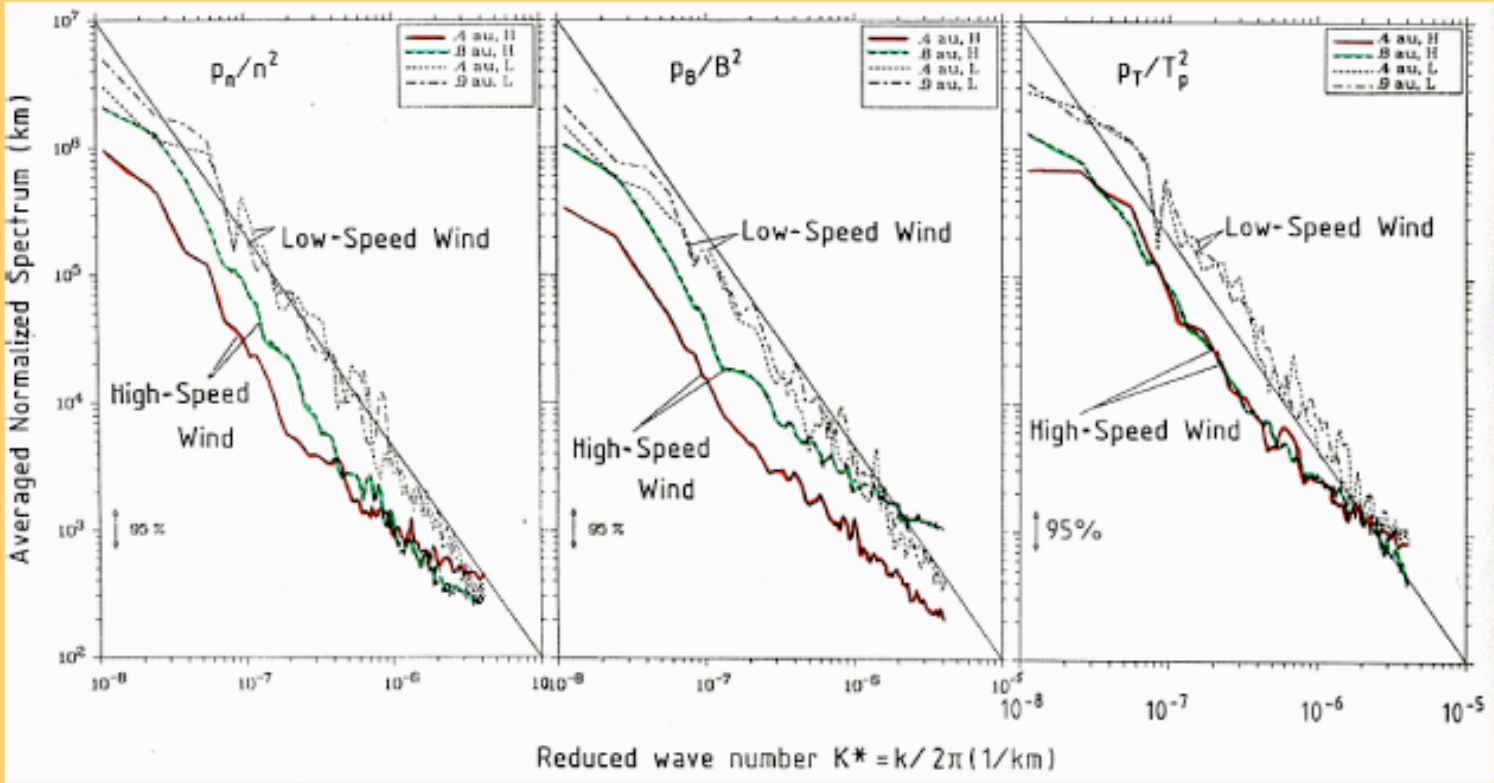

Marsch and Tu, JGR, **95**, 8211, 1990

Kolmogorov-type turbulence

Possible density profile corresponding to the spectra of fluctuations (Kellogg, 1999)

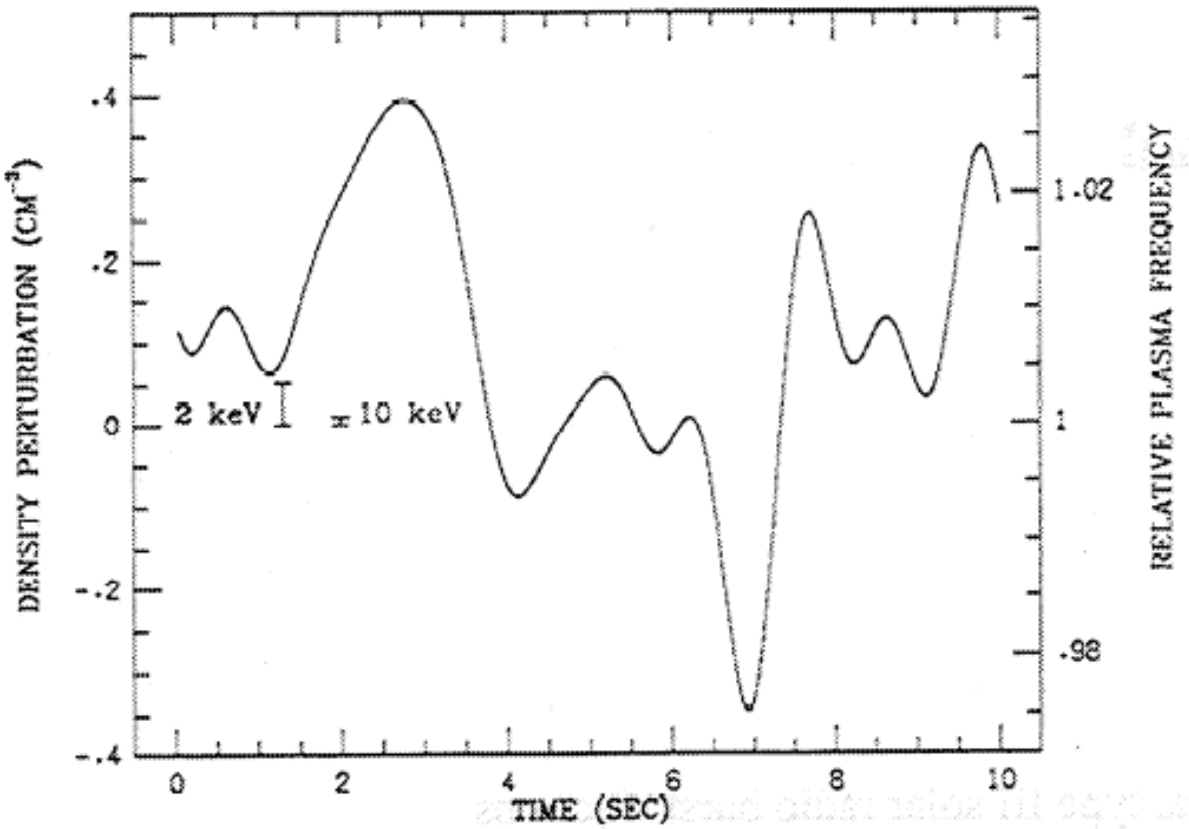

Figure 1. A time series of density fluctuations reconstructed from an averaged spectrum [*Neugebauer*, 1976]. The two brackets at the left show the difference between the plasma frequency and the resonant frequency for electron beams of 2 and 10 keV.

Critical parameters

What are the effects of inhomogeneity ?

Effect of wave propagation

- Critical parameter :
- dispersion versus density inhomogeneity, usual assumption

$$\Delta n/n \ll 3Tk^2/m\omega_{pe}^2$$

- In this case there is no wave trapping
- what will be changed if it is not correct ?

Propagation effects

- In the first case :
- random diffusion of the wavevector of the wave on the density fluctuations
- In the second case :
- a) variation of the wave amplitude due to the variations of the k-vector, and
- b) variation of the instability increment

Propagation effects

$$E(\vec{r},t) = E_0\sqrt{\frac{k_0}{k}}\exp(i\int \vec{k}(\vec{r})\cdot d\vec{r} - i\omega t + \int \gamma(t)dt)$$

WKB wave propagation, even for γ = 0

$$E \approx \frac{1}{\sqrt{k}}$$

energy flux constant

$\Delta n / n \sim 10^{-3}$

Propagation to denser plasma results in decrease of k – vector and increase of the wave amplitude, but also in wave damping on thermal electrons for HF waves

Nonhomogeneity effects

- There can be two types of inhomogeneities
- Let k-wavevector, q characteristic scale of « short scale » inhomogeneity, and Q –of « large scale » inhomogeneity
- let the conditior

$$\Gamma/v_{\mathrm{g}} \ll q \ll k.$$

- is satisfied for « large scales » and
- and the condition

$$Q < \Gamma/v_{\mathrm{g}} \ll q \ll k.$$

- for « short scales »

Historical background

- Clumping of Langmuir waves in type III solar radio burst sources (Gurnett, 1978, Smith, 1977)
- No support for collapsing solitons (Smith, 1977)
- Role of plasma inhomogeneities in suppression of the linear instability due to removal of waves from resonance (Melrose, 1980, Smith and Sime, 1979)
- Density fluctuations are present in the solar wind Neugebauer, 1975, 1976; Celniker et al., 1983, 1987

Historical background

- Nishikawa & Ryutov, (1976) two physical effects should be taken into account : angular diffusion on the small amplitude density fluctuations and growth rate
- Notion of angular averaged increment
- Muschietti et al., (1985), Breizman, Ryutov, 1980: effect of the quenching of the instability due to angular diffusion
- Robinson (1995), stochastic growth rate, importance of the analysis of PDF

Stochastic growth rate theory

(Robinson, 1995)

$$\frac{dW}{dt} = \Gamma W$$

$$G = \ln(W / W_0)$$

$$\frac{dG}{dt} = \Gamma$$

Stochastic growth rate (3)

$$\partial_t P(\Gamma,t) = \partial_\Gamma \left[k_\Gamma \left(\Gamma - \langle \Gamma \rangle_s \right) P(\Gamma,t) \right] + \frac{1}{2} D_{\Gamma\Gamma} \partial^2_{\Gamma\Gamma} P(\Gamma,t)$$

$$P(\Gamma,t) = \frac{1}{\sigma(\Gamma,t)\sqrt{2\pi}} \exp\left(- \frac{\left(\Gamma - \langle \Gamma(t) \rangle \right)^2}{2\sigma^2(\Gamma,t)} \right)$$

This theory is asymptotic and it is based on the central limit theorem:

Number of regionds of growth and damping should be very large

Basic model

- Similar to Nishikawa & Rytov (1976)
- Two effects: angular diffusion and linear growth rate / damping

Basic model

$$Q < \Gamma / v_g << q << k$$

$$1/qv_g << \Delta t << 1/\Gamma, 1/Qv_g$$

$$1/q << \Delta r << v_g/\Gamma, 1/Q$$

$$\Delta n/n << k^2 T/m\omega_{pe}^2 \sim \Delta N/n$$

Equation for the spectral energy density of the Langmuir wave packet moving in plasma with random inhomogeneities

$$v_{gr}\cos\theta\frac{\partial W(\theta,x)}{\partial x}=\frac{1}{\sin\theta}\frac{\partial}{\partial\theta}\left(D(\theta,x)\sin\theta\frac{\partial W(\theta,x)}{\partial\theta}\right)+\gamma(\theta,x)W(\theta,x)$$

Angular diffusion

Growth inside the resonant region, damping outside it

Langmuir wave propagating in a plasma with a density gradient

$$k^2(x) = \frac{\omega^2}{3\lambda_D^2 \omega_p^2(x)} - \frac{1}{3\lambda_D^2};$$

$$\omega_p^2(x) = \frac{4\pi \bar{n}_e e^2}{m_e};$$

$$\lambda_D^2 = \frac{kT}{4\pi \bar{n}_e e^2}.$$

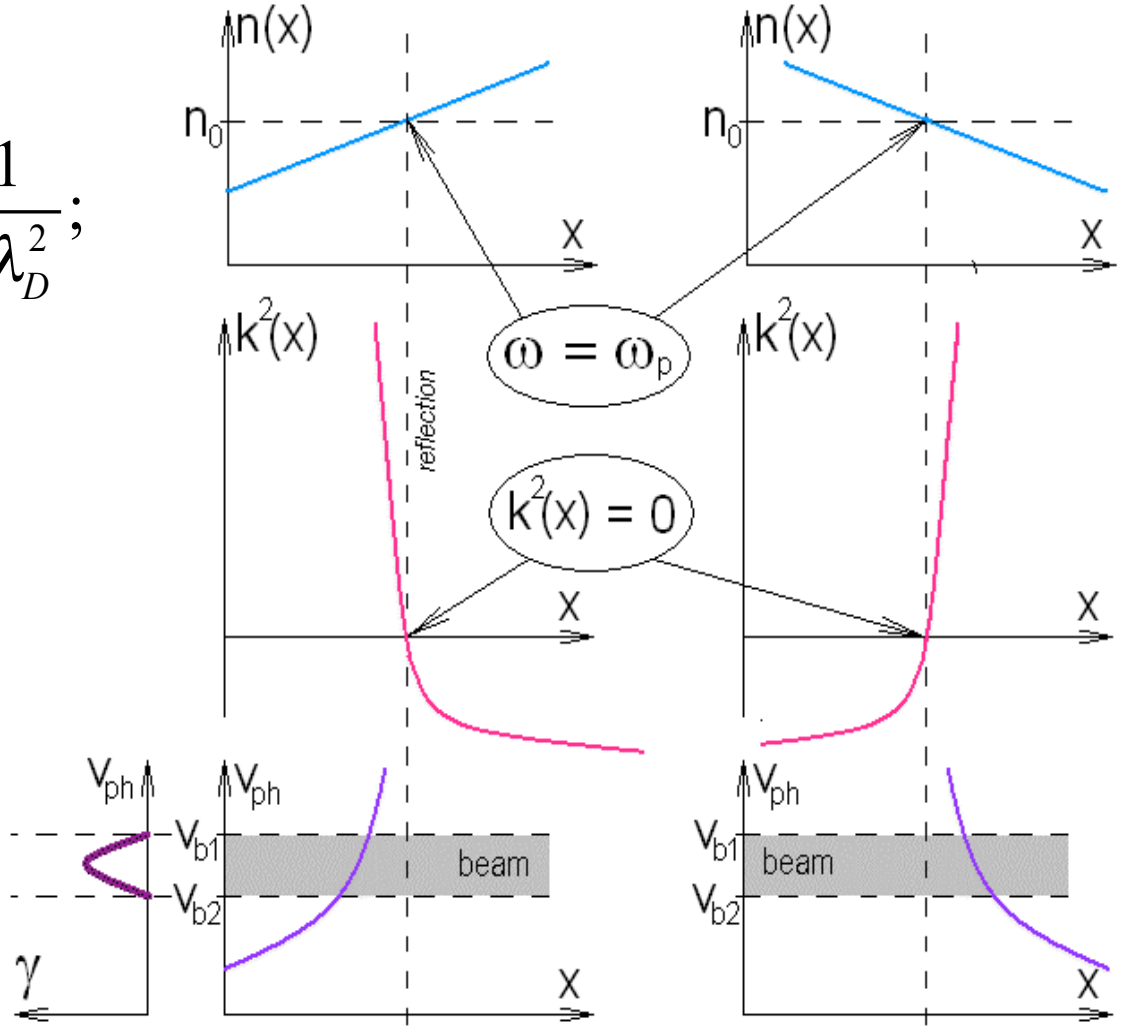

Competition between growth and angular diffusion

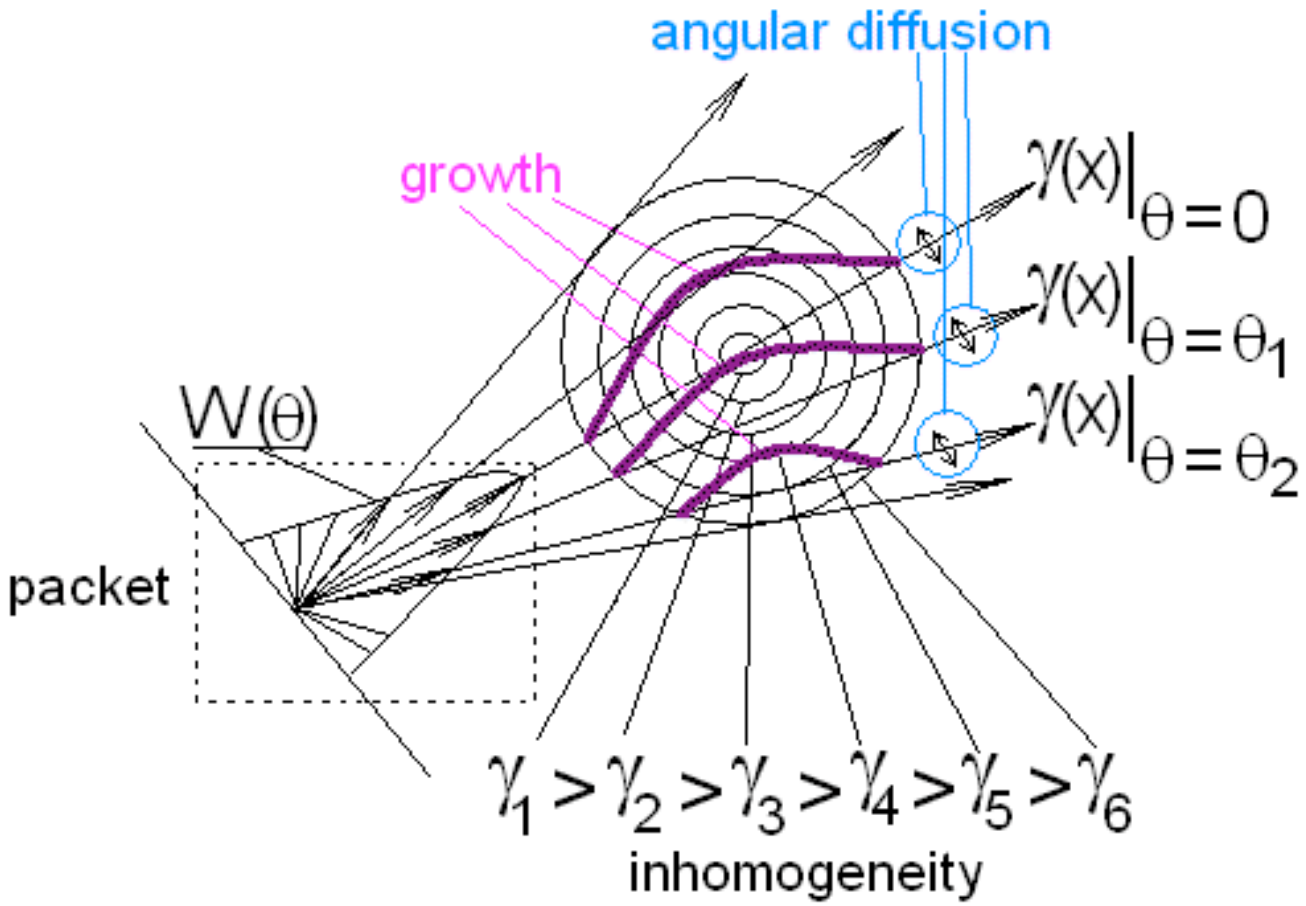

Spatial distribution of the growth rate

$$\gamma(x,\theta) = \gamma_0 x(x_{\max} - x)/(x_{\max}/2)^2 \cos\theta - \gamma_{\pi/2}$$

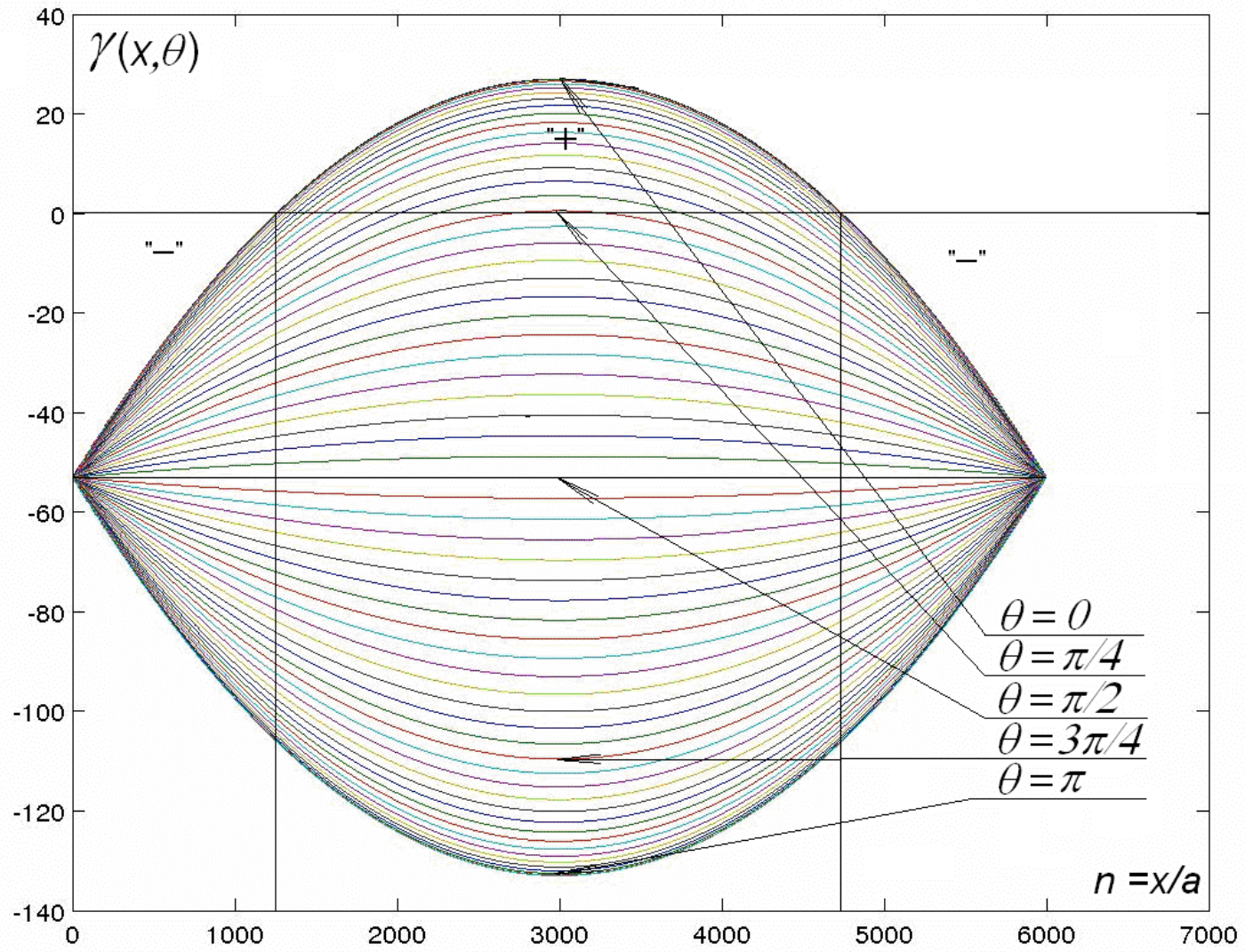

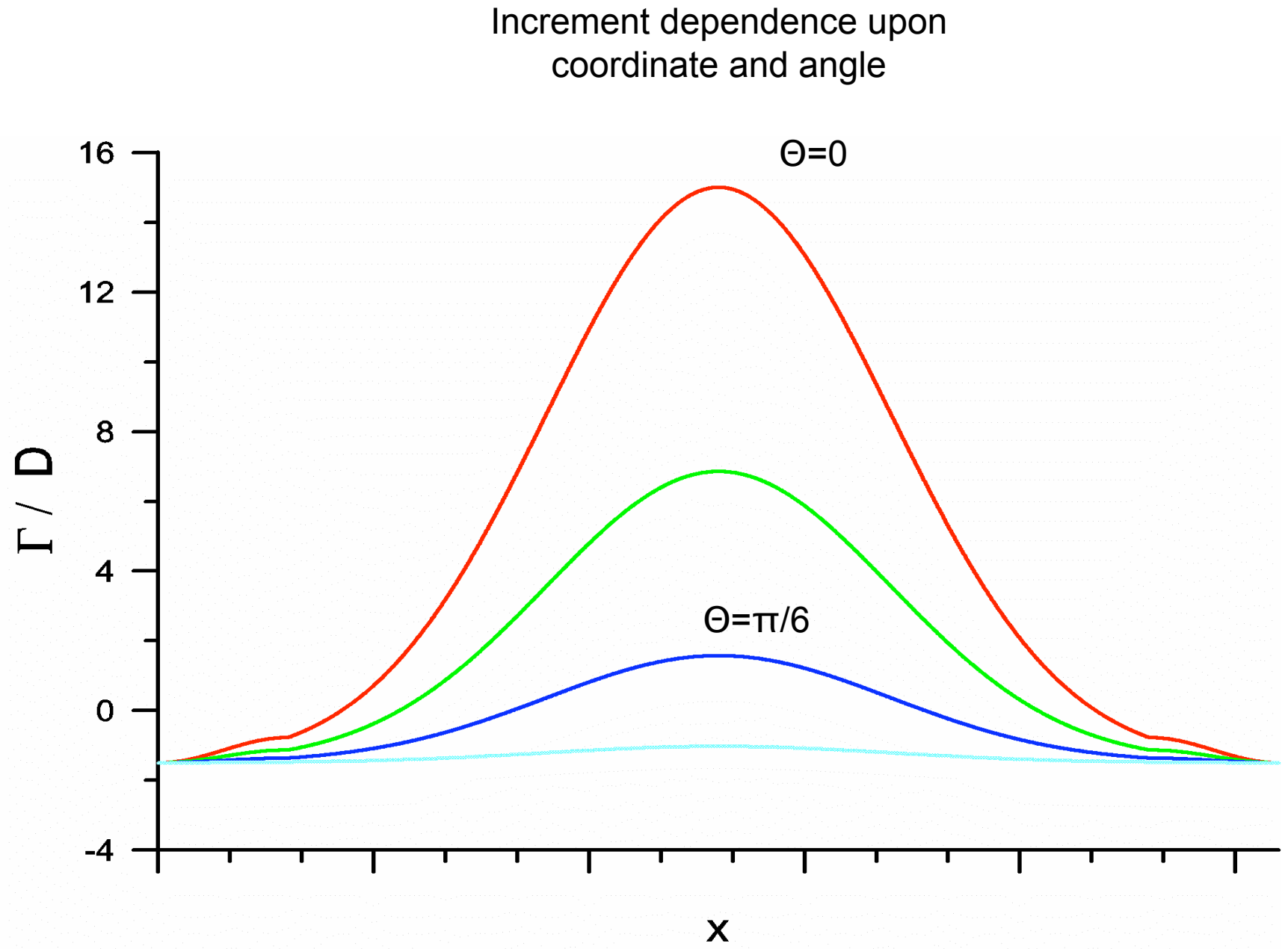
Increment dependence upon
coordinate and angle
Θ=0
Θ=π/6
16
12
8
4
0
-4
Γ / D
x

Equation

$$\frac{d^2W(\theta,x)}{d\theta^2}+\cot\theta\frac{dW(\theta,x)}{d\theta}-[W(\theta,x+\Delta x)-W(\theta,x)]\delta_1\delta_2\cos\theta+$$

$$+W(\theta,x)\delta_1[\frac{x(x_{\max}-x)}{(x_{\max}/2)^2}\cos\theta-\frac{\gamma_{\pi/2}}{\gamma_0}]=0$$

Thomas method

Numerical modeling with a single large-scale inhomogeneity

$$\frac{\Gamma(x,\theta)}{\Gamma_{\max}} = -0.1 + 1.1 \exp\left[-\frac{1}{2}\left(\frac{\theta}{\Delta\theta}\right)^2\right] \exp\left[-\frac{1}{2}\left(\frac{x - x_0}{\Delta x}\right)^2\right]$$

Spatial distribution of the spectral energy density

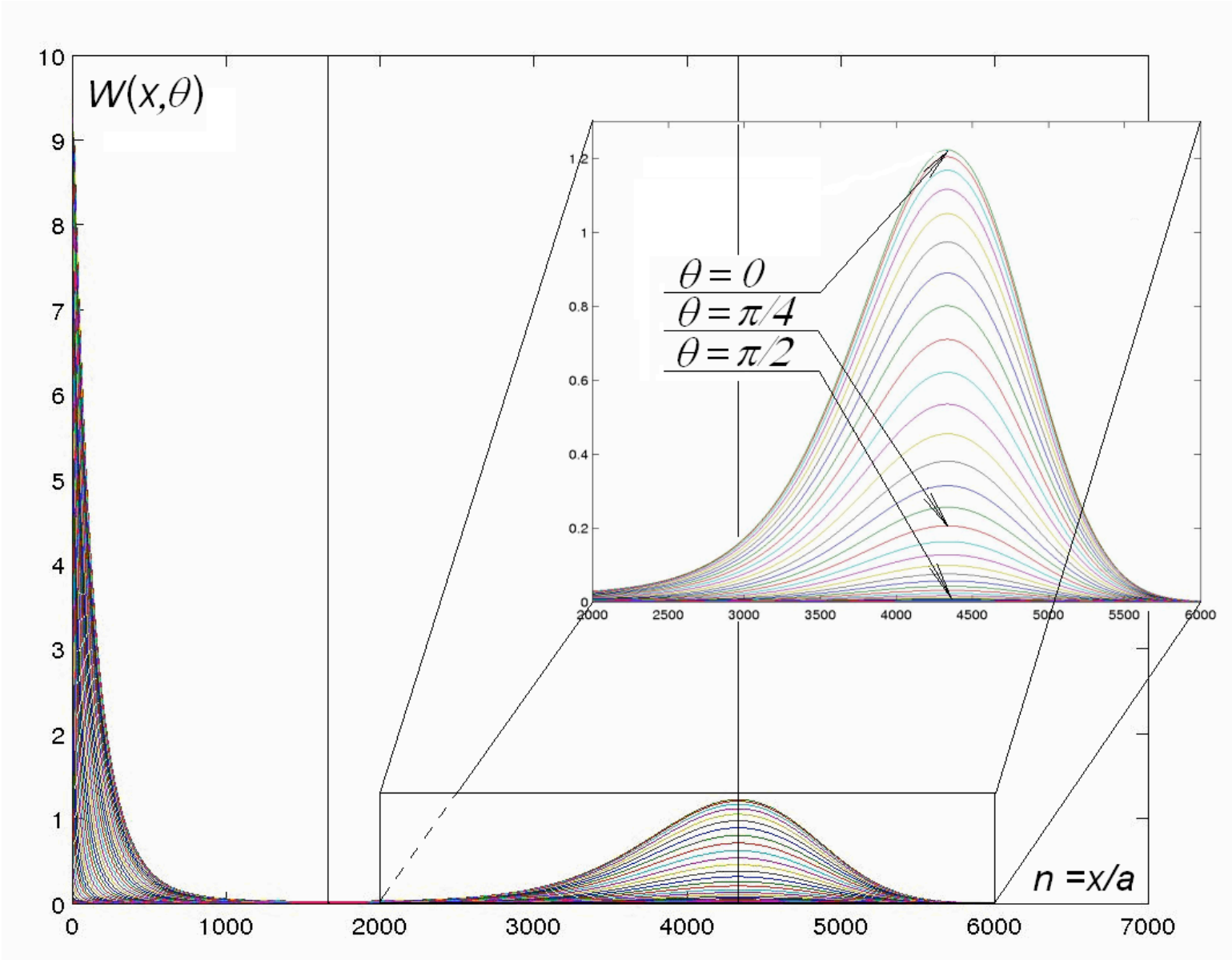

The results of numerical simulations with a single large-scale inhomogeneity.

(a) Spatial profiles of the ratio Γ/D for $\theta = 0$ and $\Gamma_{max}/D = 10, 15, 20$.

(b) Spatial dependence of normalized wave energy densities.

(c) The profiles from (b) after a spatial shifts.

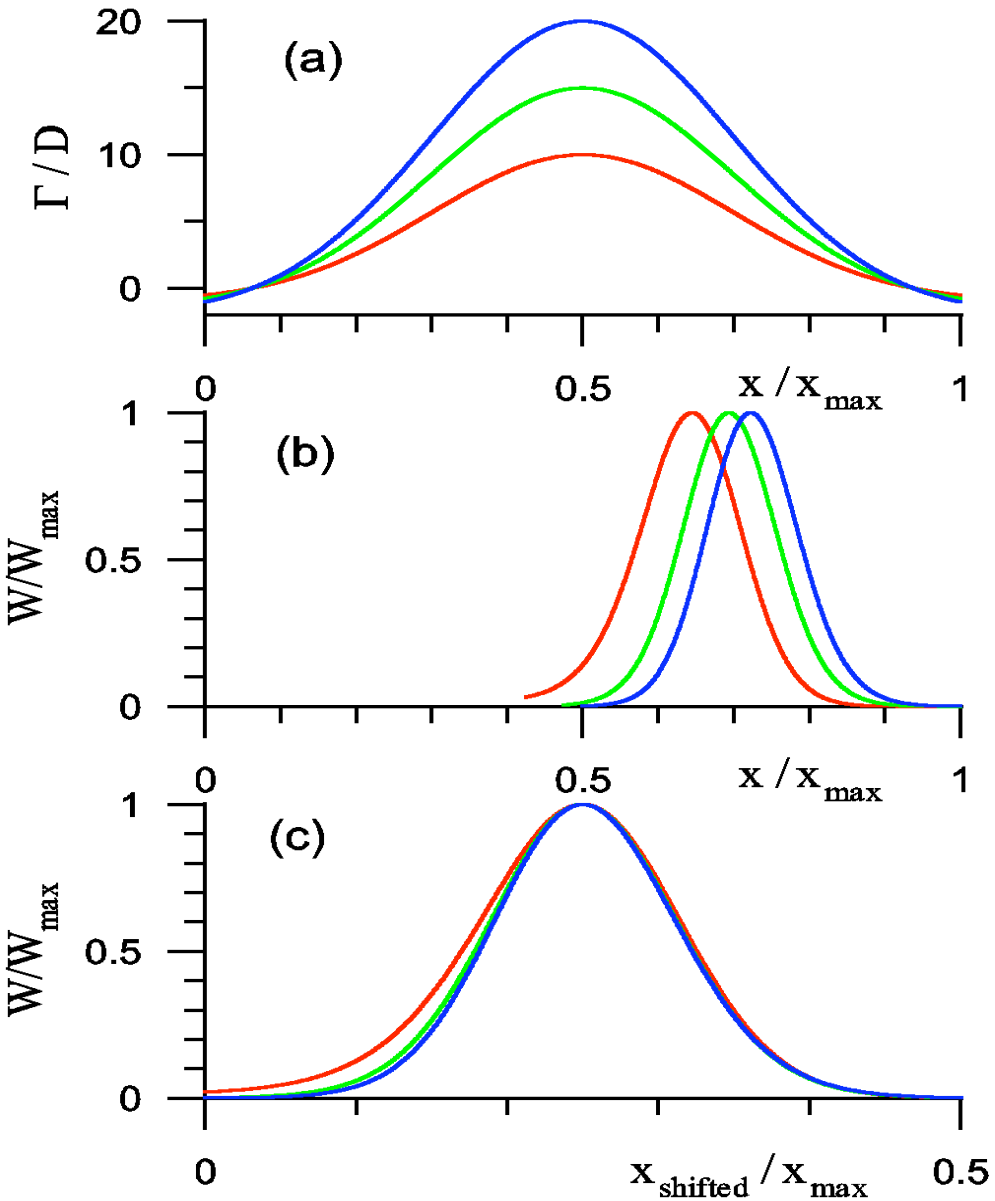

Characteristic growth rate dependence upon parametres

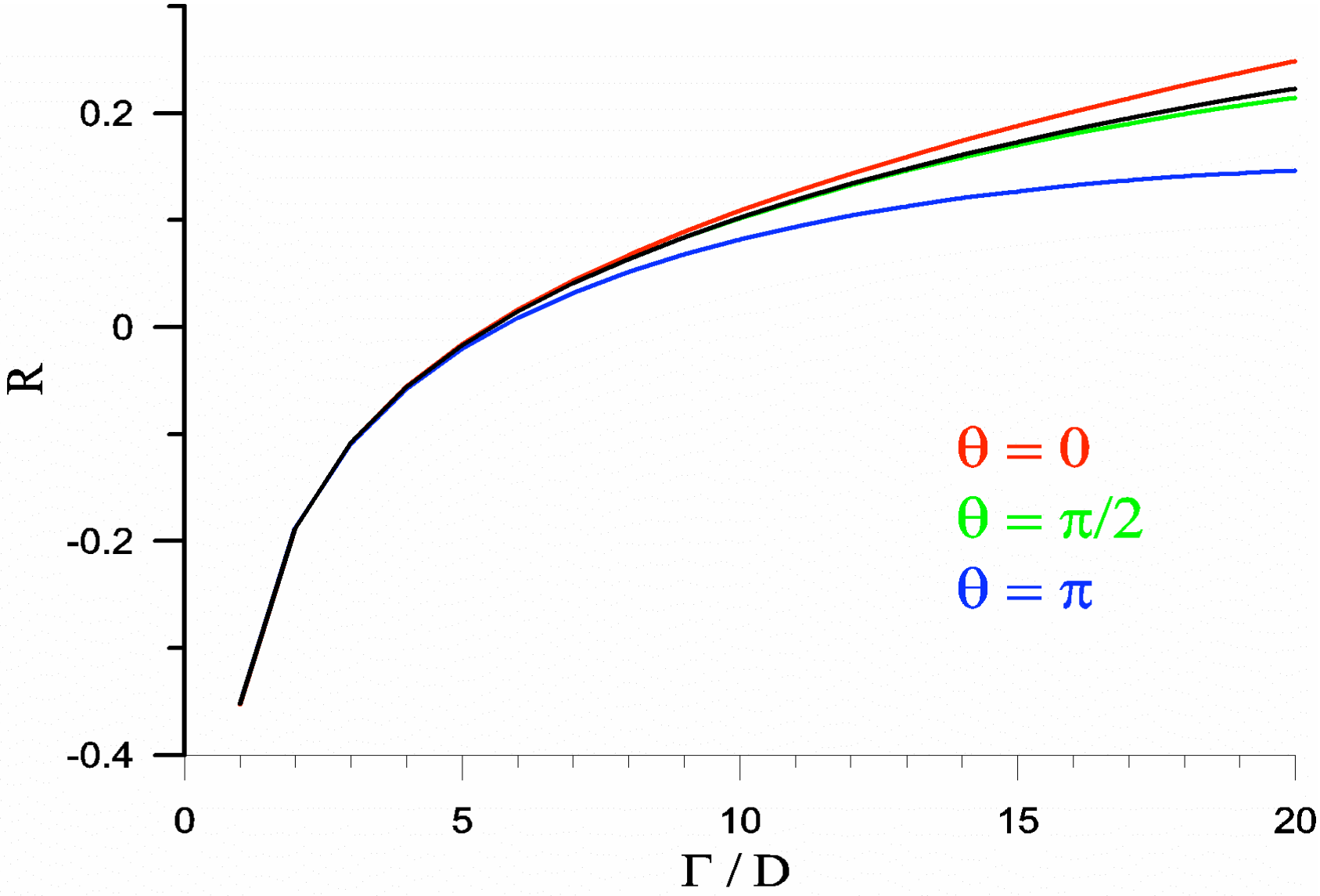

Numerical modeling with several random inhomogeneities

$\Gamma(x,\theta)$ is a noise-like function containing random number of pulses with random amplitudes and positions

10000 runs

Problem of characterization of the shot noise

Rice (1944), Gilbert & Pollak (1960)

For impulse shapes F(t) the probability distributions

$$Q(I) = \Pr[I(t) < I]$$

obey an integral equation

$$IQ(I) = \int_{-\infty}^{t} Q(x)dx + n\int_{-\infty}^{\infty} Q[I - F(t)]F(t)dt$$

n – the average number of pulses per unit of time

Examples

1. Step-like distribution with the amplitude b, and average pulse rate n

$$\Pr[I(t) = kb] = \frac{(nA)^k}{k!}\exp(-nA)$$

2. F(t) = (1 – t), on time interval 0 < t <1, pulse rate n

$$P(I) = \exp(-n)\sum_{k=0}^{I}\frac{(-1)^k}{k!}n^{k+1}(I-k)^{(k+1)/2}I_{k-1}[2\sqrt{n(I-k)}],$$

Exponential distribution

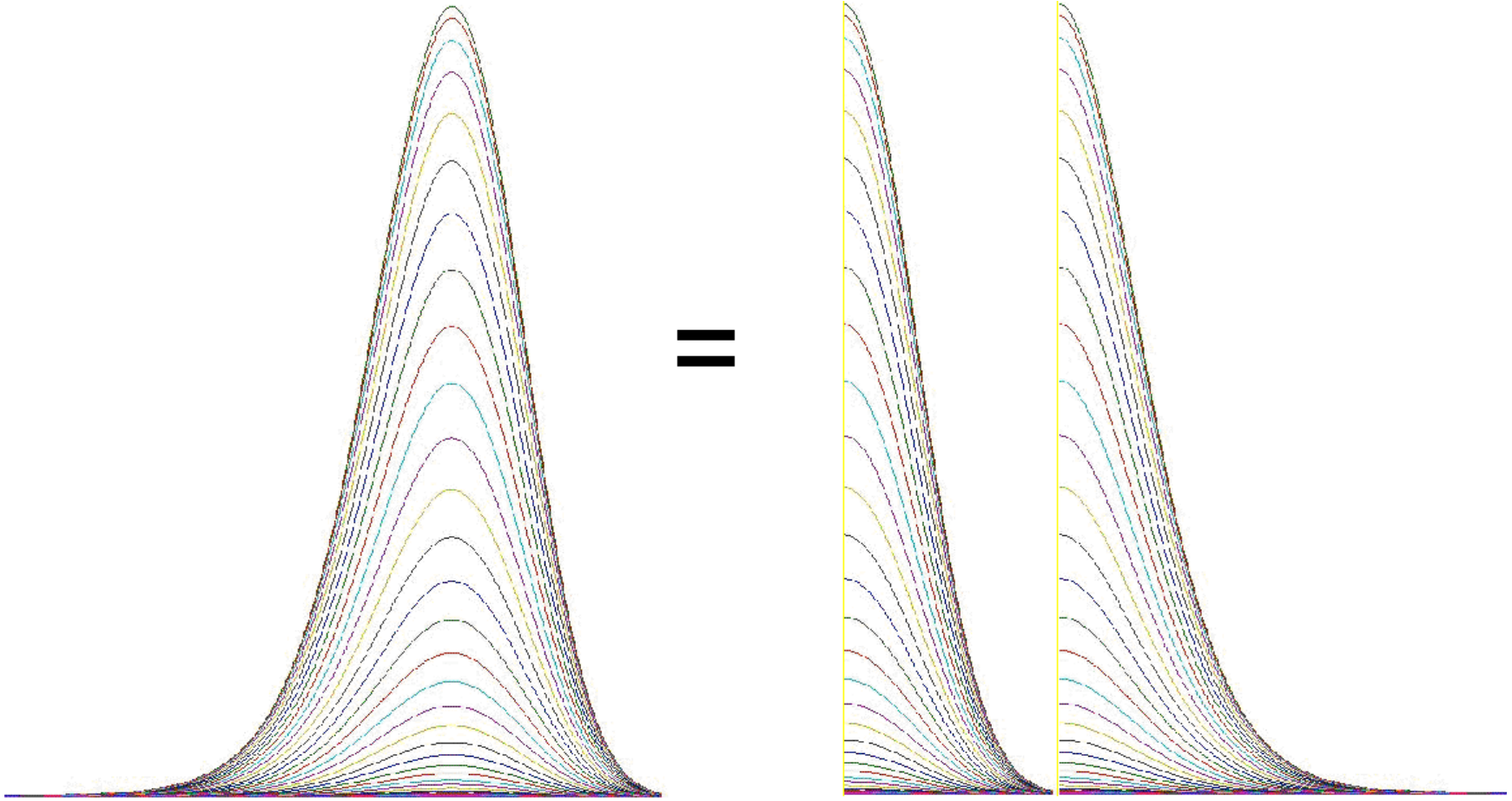

Probability distribution function for shot noise with exponential pulses (Gilbert and Pollak, 1960)

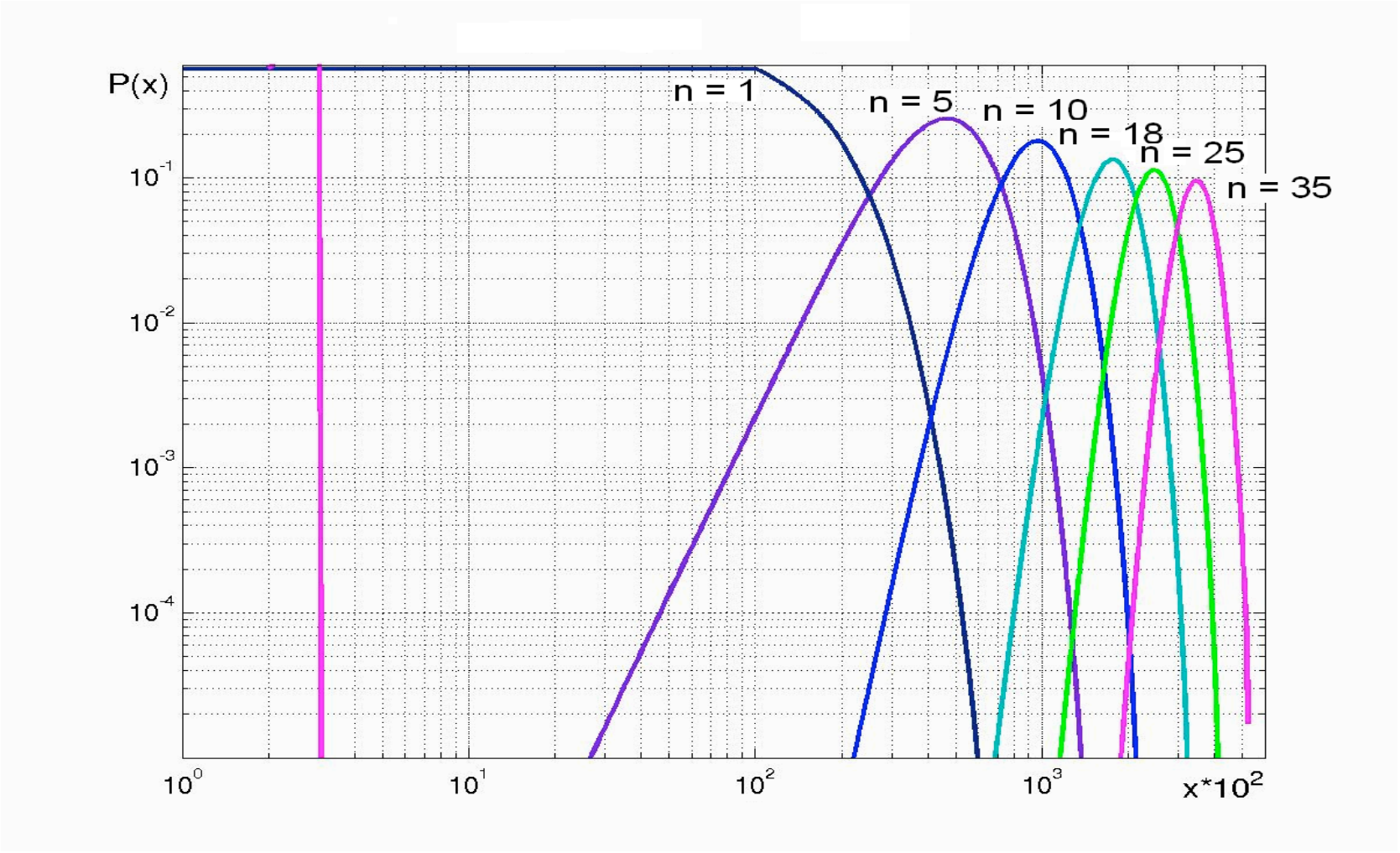

How to compare model distributions with experimental ones ?

Pearson classification of distributions:

Gamma, beta, normal, log-normal et cetera
Belong to these classes. Two parameters that
Characterize the distribution family:

are related to skewness and curtosis

Some definitions

$$g_1 = \mu_3 / \mu_2^{3/2} = \beta_1^{3/2}$$

G_1 and G_2 are unbiased estimates of g_1 and g_2

Position on the diagram for Pearson curves

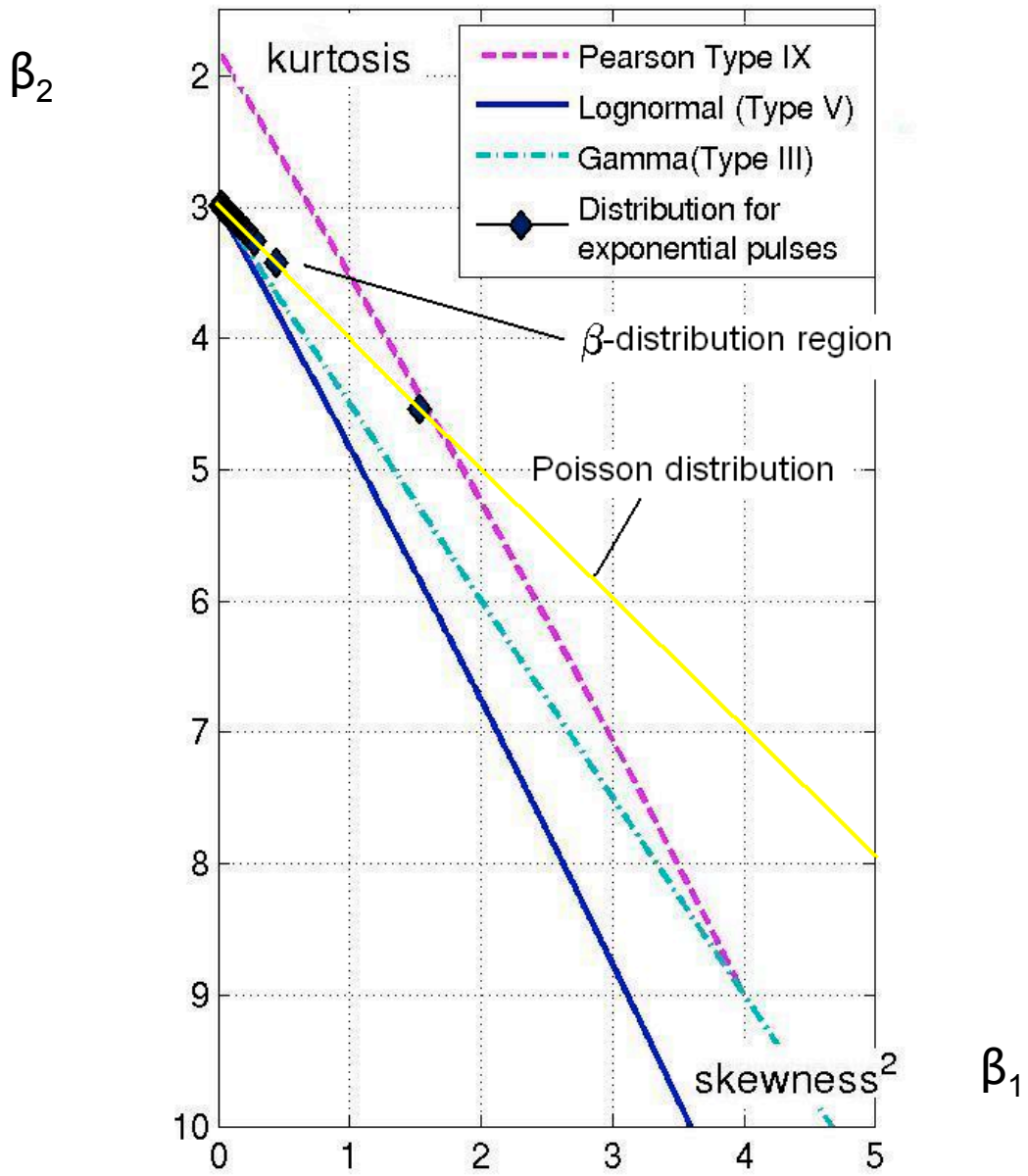

Statistical characteristics

Two factors:

- The form of the distribution (exponential)
- The statistics of increment distribution

(Gaussian)

Dependence of G_1 and G_2 on the effective number of regions with the positive growth rate

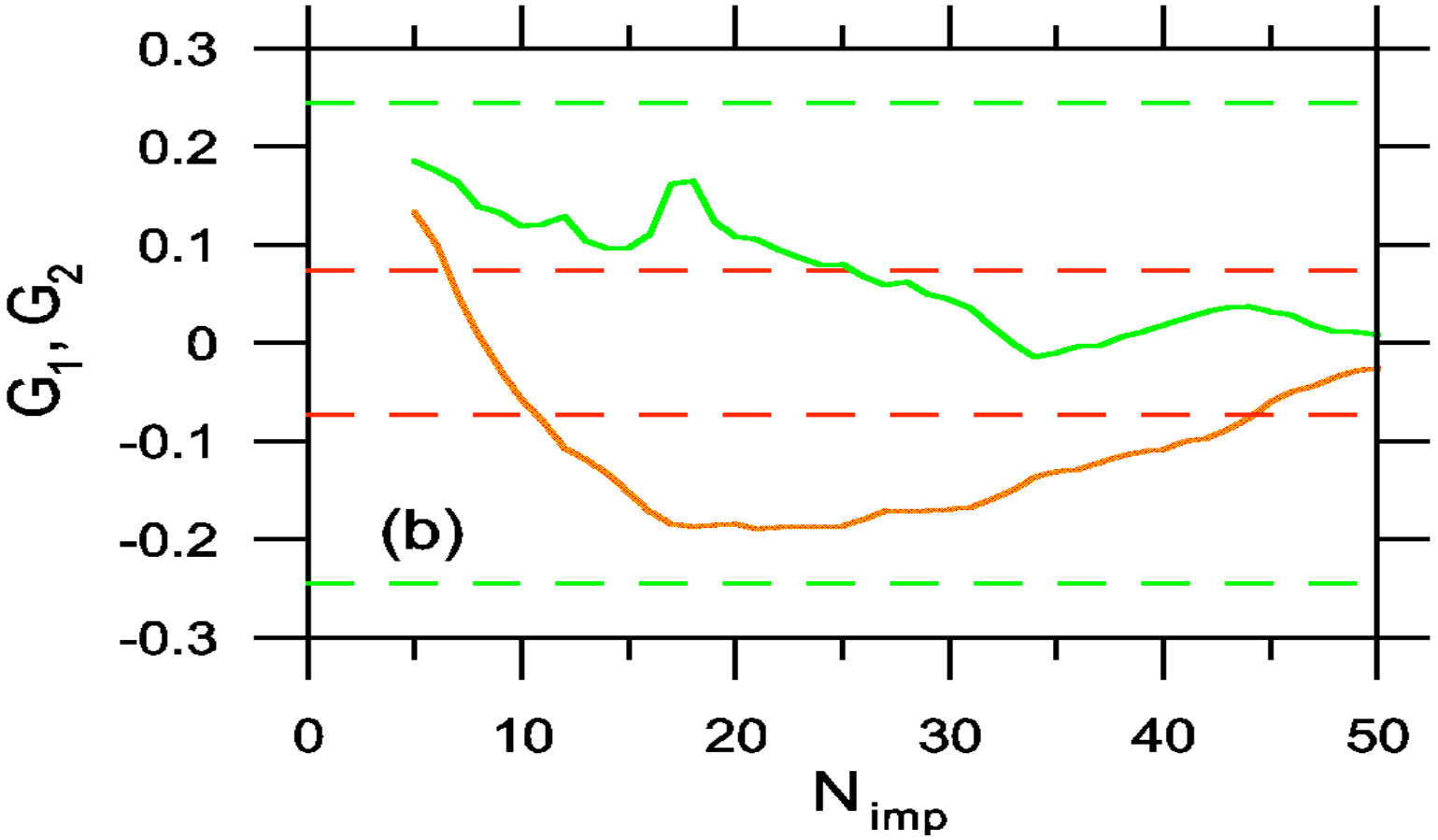

Probability distribution function of wave amplitudes

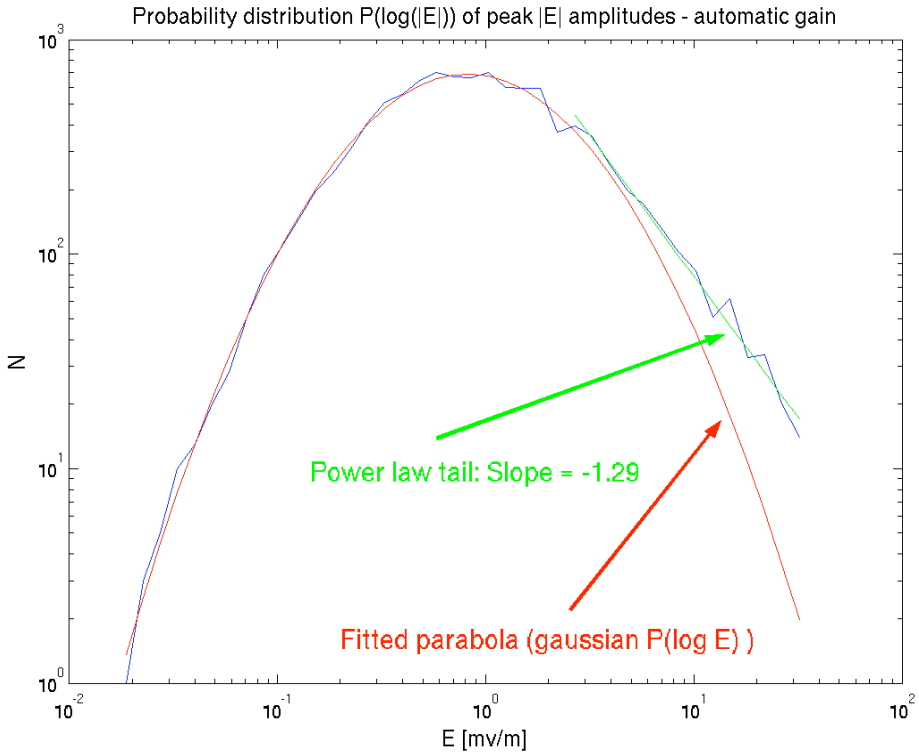

In this viewgraph is plotted the PDF of peak wave amplitudes P(log E) in log-log axes (based on foreshock event from Feb 17, 2002). The amplitudes seem to be distrubuted similar to beta / gamma or log-normal PDF with a power-law tail at largest amplitudes. We suggest that the physics of large amplitude waves might be different from the physics at low amplitudes.

Experimental data overview

- **High frequency electric field data from the WBD instrument of CLUSTER**
- **Measures one component of the E-field**
- **Band-pass filtered between 1 kHz and 77 kHz**
- **WBD operates in duty cycles - each block of data is 10 milliseconds long and is followed by a gap of 80ms. The size of this block imposes limits the spectral resolution of the Fourier transform.**

The Event (March 16, 2001)

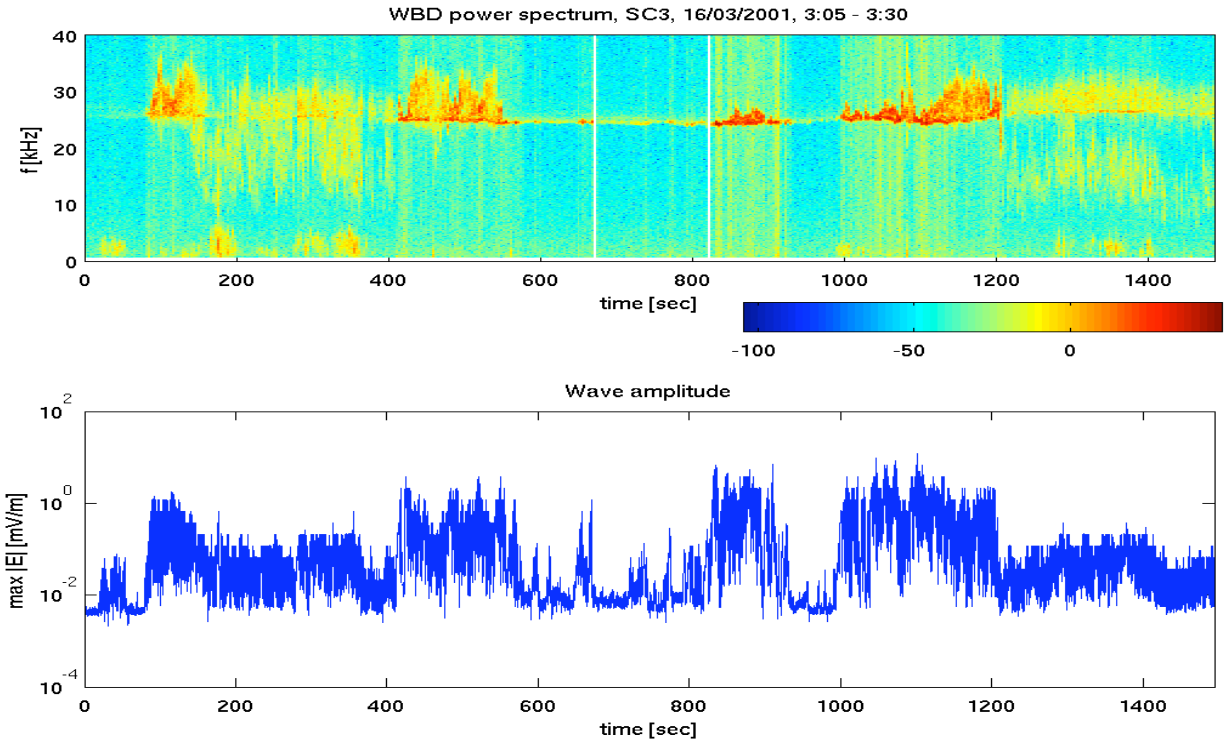

- **CLUSTER in the Earth‘s foreshock (Diff = 0 .. - 6 R_E)**
- **Observed wave amplitudes up to 5 mV/m**

Typical waveform

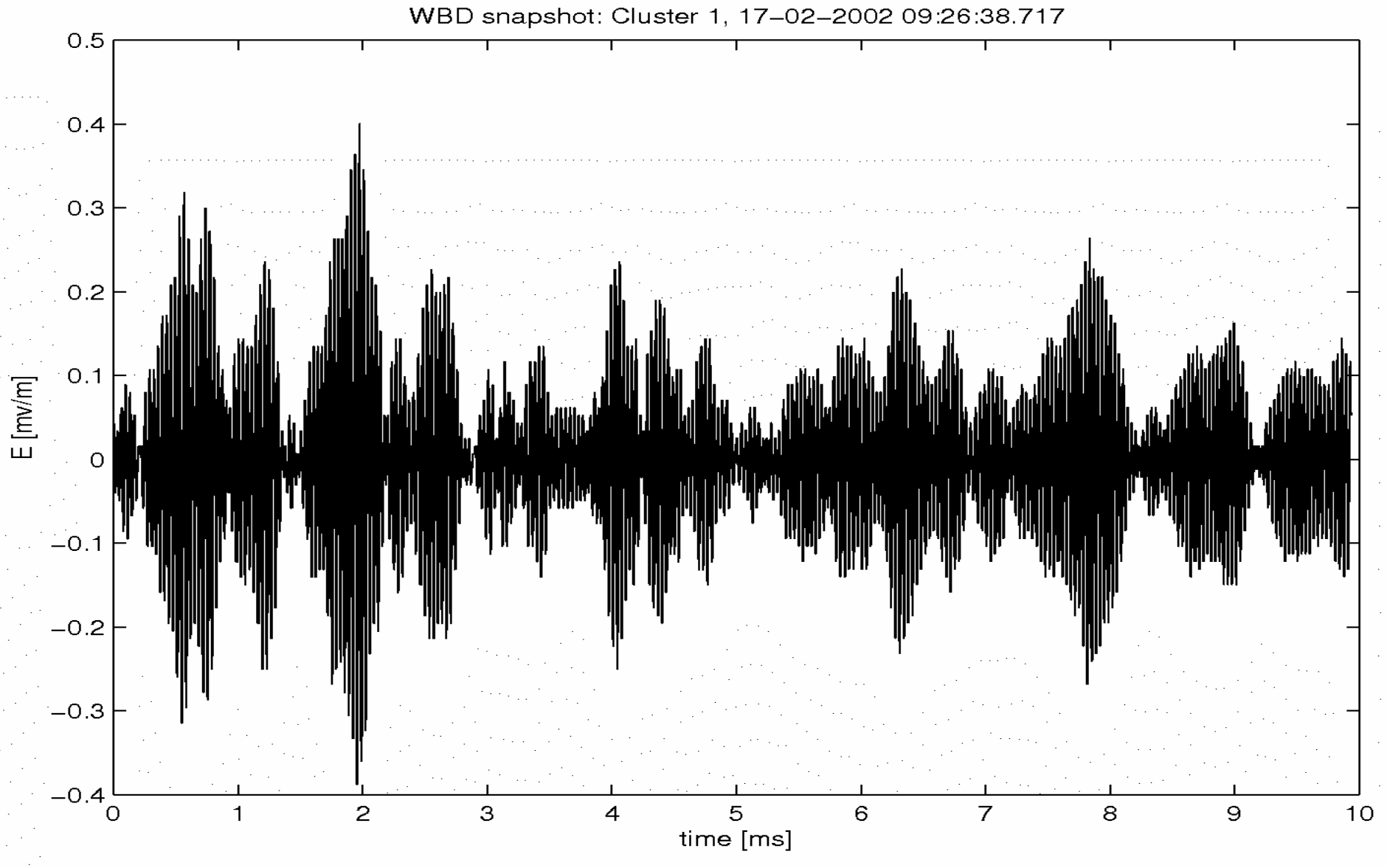

Data processing

- Correction of measured amplitudes to take into account antenna position with respect to magnetic field
- Removing data with strong instrumental effects and large angle between antenna and magnetic field (> 75 deg)

Ensemble of more than 22000 values of mean $|E|^2$

PDF for Langmuir wave energy density for the period 9:25-10:13 UT on February 17, 2002

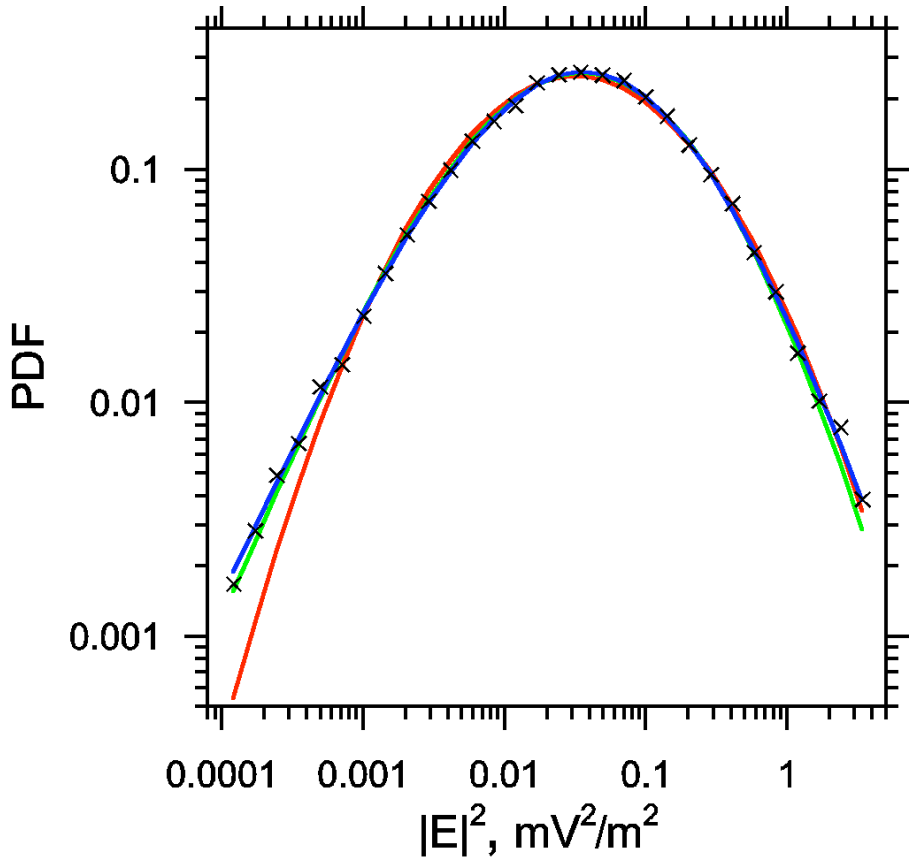

x – experiment

—— maximum likelihood fit of a log-normal distribution

—— fit of Pearson class IV distribution obtained by maximum likelihood method

—— fit of Pearson class IV distribution with parameters derived from estimates of moments

Pearson type IV distribution

Probability distribution fit of the WBD data (13 May 2002)
Amplitudes 0.012 - 0.400 mV/m, num. samples = 25328, num. bins = 30

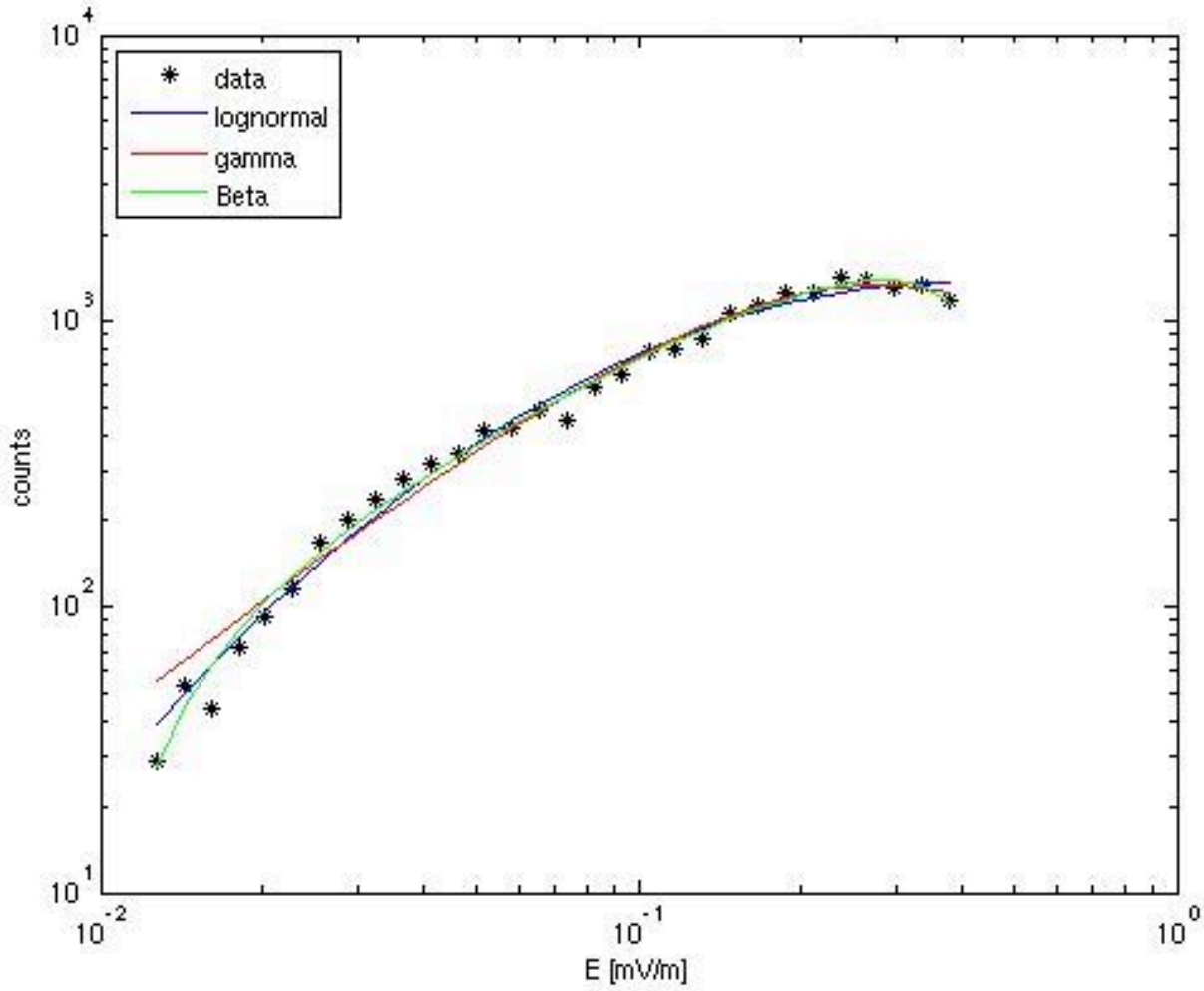

Log-normal-distribution : χ^2-Maximum Likelihood : 154.70, α = 1.000000

Gamma-distribution : χ^2-Maximum Likelihood : 128.69, α = 1.000000

Type IV Pearson-distribution : χ^2-Maximum Likelihood : 67.37, α =0.999995

Results of analysis of Whisper data

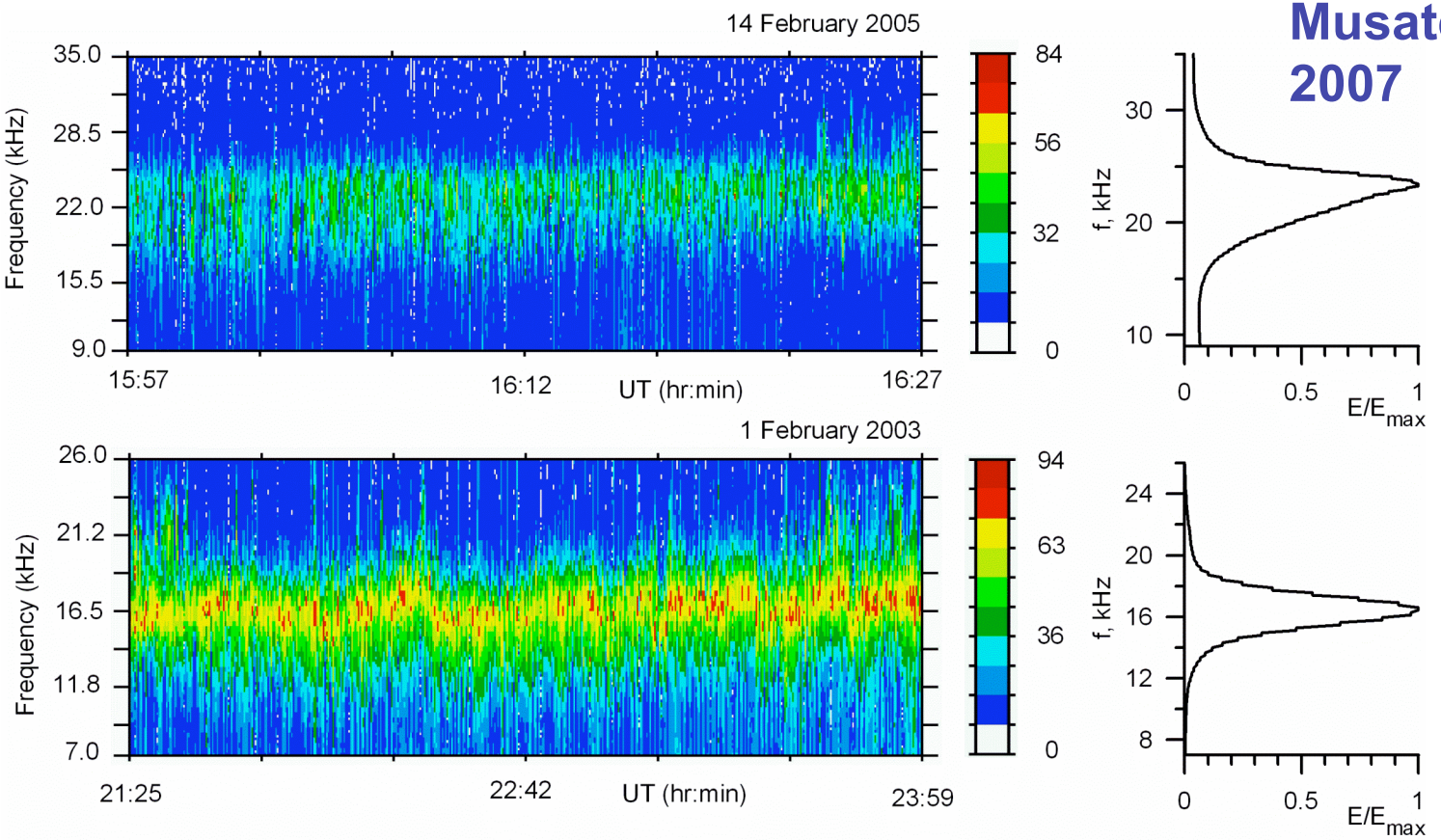

Musatenko et al., 2007

- **Figure 1. Frequency-time spectrograms obtained by the WHISPER instrument in the Earth's electron foreshock on 1 February 2003 and 4 February 2005 (from top to bottom). The electric field strength is expressed in Vrms Hz-1/2, the signal level is color coded and plotted in dB over 10-7 Vrms Hz-1/2. The corresponding color scales are shown on the right of the spectrograms. Right panel contains the spectra averaged over the entire time interval.**

Results of analysis of Whisper data

(Musatenko et al., 2007)

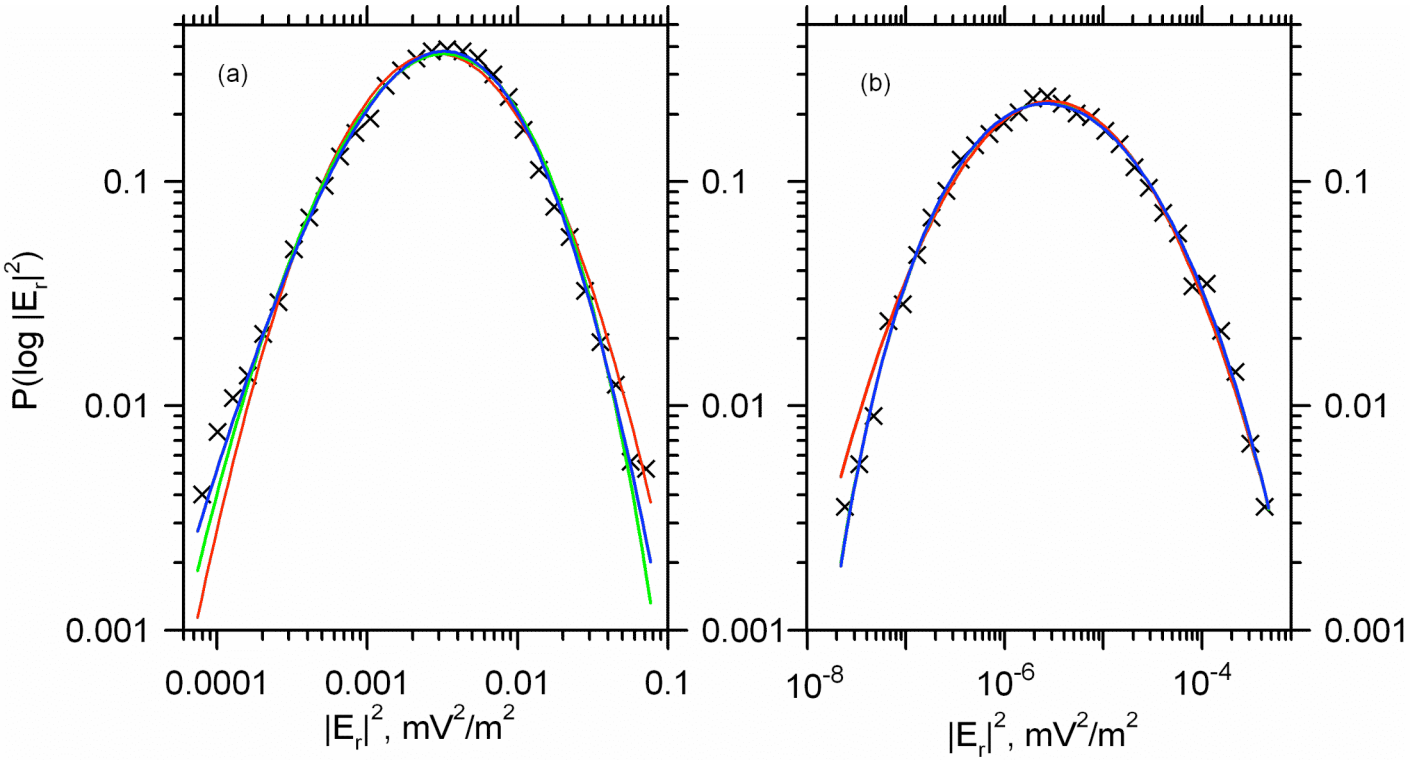

- Figure 2. Probability density function for logarithm of energy density of Langmuir waves observed
- (a) during 21:25-24:00 UT on 1 February 2003 and
- (b) during 15:57-16:27 UT on 14 February 2005,
- when CLUSTER spacecraft were within the Earth's electron foreshock (black crosses). The red line shows the maximum likelihood fit by normal distribution. The green and blue lines correspond to fits of Beta distribution and Pearson Type IV distribution, respectively.

Diagram for various types of Pearson distributions

(red circles - numerical simulations;
green cross - experimental data)

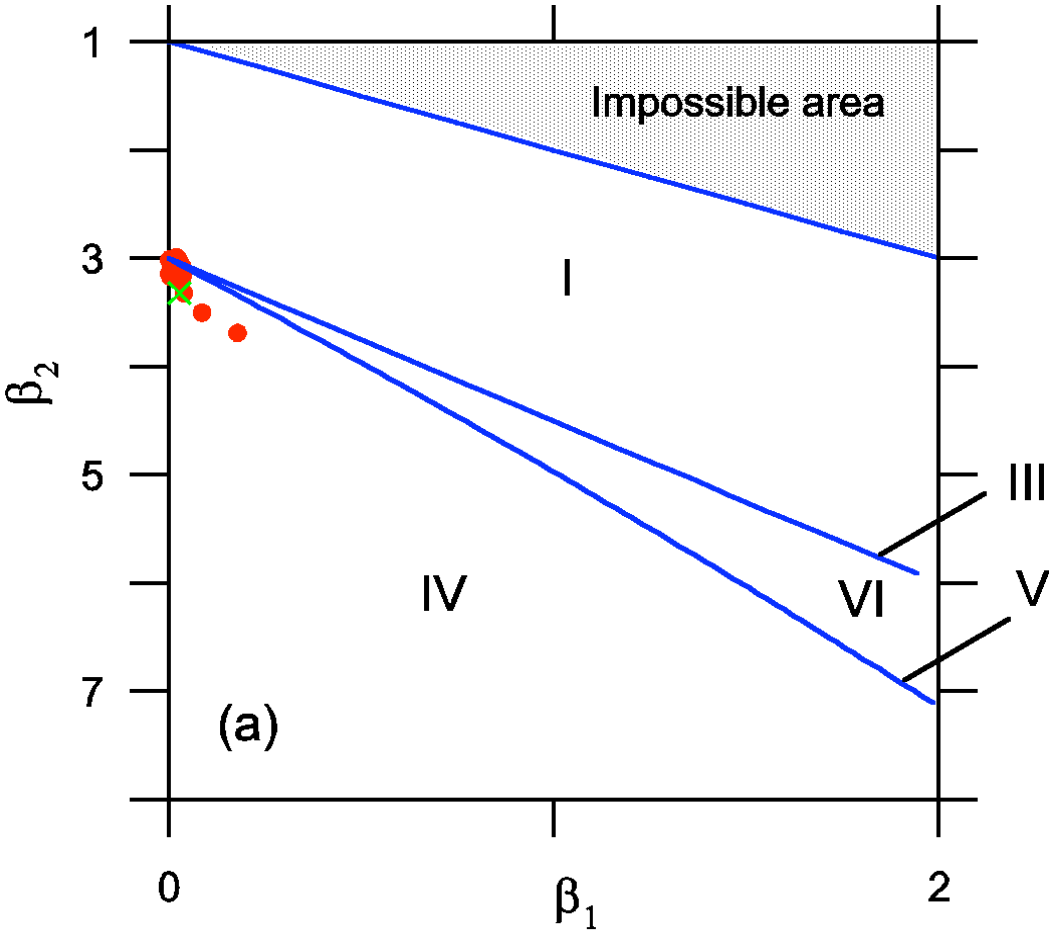

Conclusions

- We consider the model describing the interaction of Langmuir wave packets with the beam in a randomly inhomogeneous plasma. Two effects are taken into account:

  angular diffusion of the wave vector on the small amplitude density fluctuations,

  the suppression of the instability caused by the removal of the wave from the resonance with particles crossing density perturbations of relatively large amplitude

- The problem is similar to the description of the shot noise and can be statistically treated in a similar way
- The major characteristic features of the electric field amplitude dynamics resemble ones resulting from exponential growth / damping of wave packets
- Shot noise consisting of randomly growing / damping wave packets is described by the PDF that belongs to type IV Pearson-distributions
- The best fit to experimental data PDF's for regions, where the amplitudes of wave packets are relatively small, belongs to the same type of Pearson distributions.

Results in press:

- Krasnoselskikh, V., V. Lobzin, K. Musatenko, J. Soucek, J. Pickett, and I. Cairns, “Beam-plasma interaction in randomly inhomogeneous plasmas and statistical properties of small-amplitude Langmuir waves in the solar wind and electron foreshock”, JGR, accepted, 2007
- Musatenko et al., Statistical properties of small amplitude Langmuir waves in the Earth’s electron foreshock, Planetary and Space Science, accepted, 2007

Beam-plasma interaction in the solar wind and in electron foreshock region II

- **Nonlinear effects (probably)**

Basic properties

- Wave particle interaction in the presence of finite amplitude low frequency waves
- The maximum increment is not determined anymore by calculation of the increment taking HF pump wave and considering LF wave and another HF wave as secondary waves
- The process is localized around reflection points

Polarisation properties of high frequency waves near the electron foreshock : WIND observations and interpretation

T. Dudok de Wit, V. Krasnoselskikh
LPCE / CNRS-University of Orléans, France
S. Bale
SSL, UCB, Berkeley, California, USA

Abstract

The **electron foreshock** exhibits wind a variety of nonlinear phenomena, among which wave-wave interactions around the plasma frequency have received much interest [1,2].

A conspicuous feature is the occurrence of coherent quasi-monochromatic wave packets with close frequencies. Although these spectra are supposed to be the signature of the **nonlinear decay of Langmuir waves**, many open questions remain.

Here we consider their polarisation properties to shed a light on their interpretation. Our analysis is based on high-frequency electric field measurements made in the terrestrial electron foreshock by the WIND satellite. Two components of the electric field are available. Using a **demodulation technique**, we show how to extract the polarisation properties of the waves and compare these to the orientation of the magnetic field.

The main observed feature is a **quasi co-planarity of the k-vectors** of the primary and secondary waves, and their closeness to the direction of the background magnetic field. These results give a strong argument in favour of the theoretical model of beam-plasma interaction, where the saturation of the wave amplitude is determined by the decay instability. This is further supported by the orientation of the k-vector of the secondary wave, which is

Context

- The electron foreshock exhibits highly coherent wave packets with two close frequencies

Kellogg et al. J GR 102 (1997)

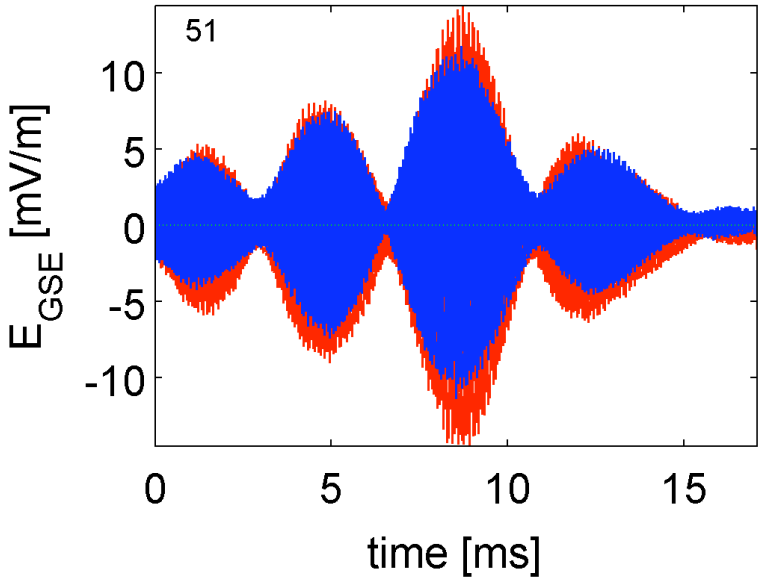

Objective

- These waves are expected to result from the **nonlinear decay** of intense Langmuir wave packets, yet their origin is still debated.

- We measured the **polarisation** and the **k-vector** of the individual interacting waves.

- Our results provide experimental

Typical waveform

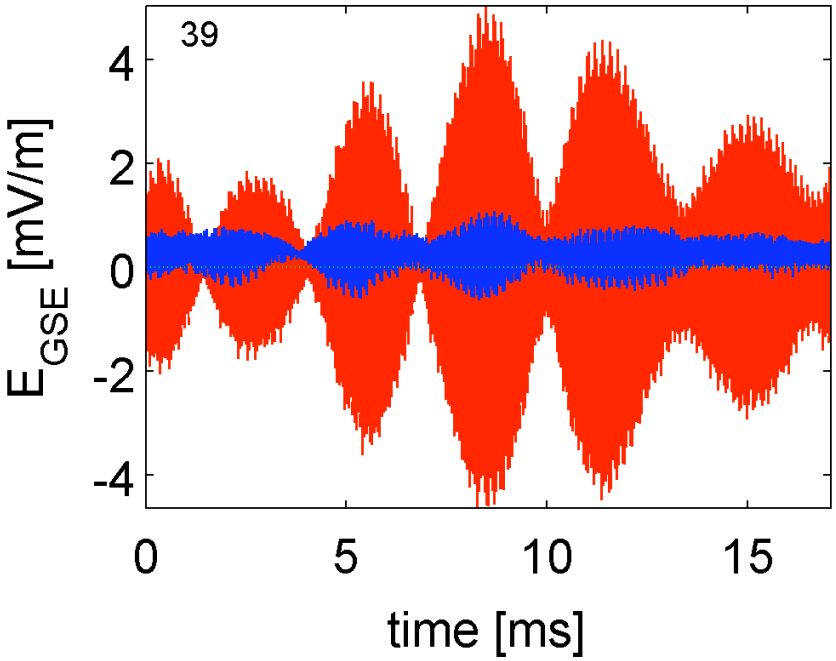

Electric field
(E_X and E_Y)

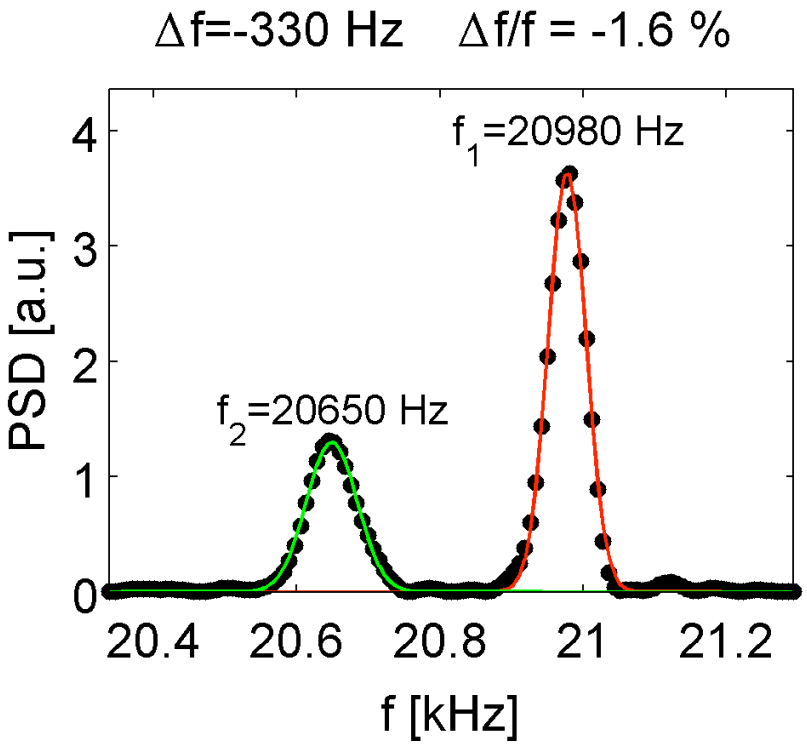

Power Spectral Density

Other examples

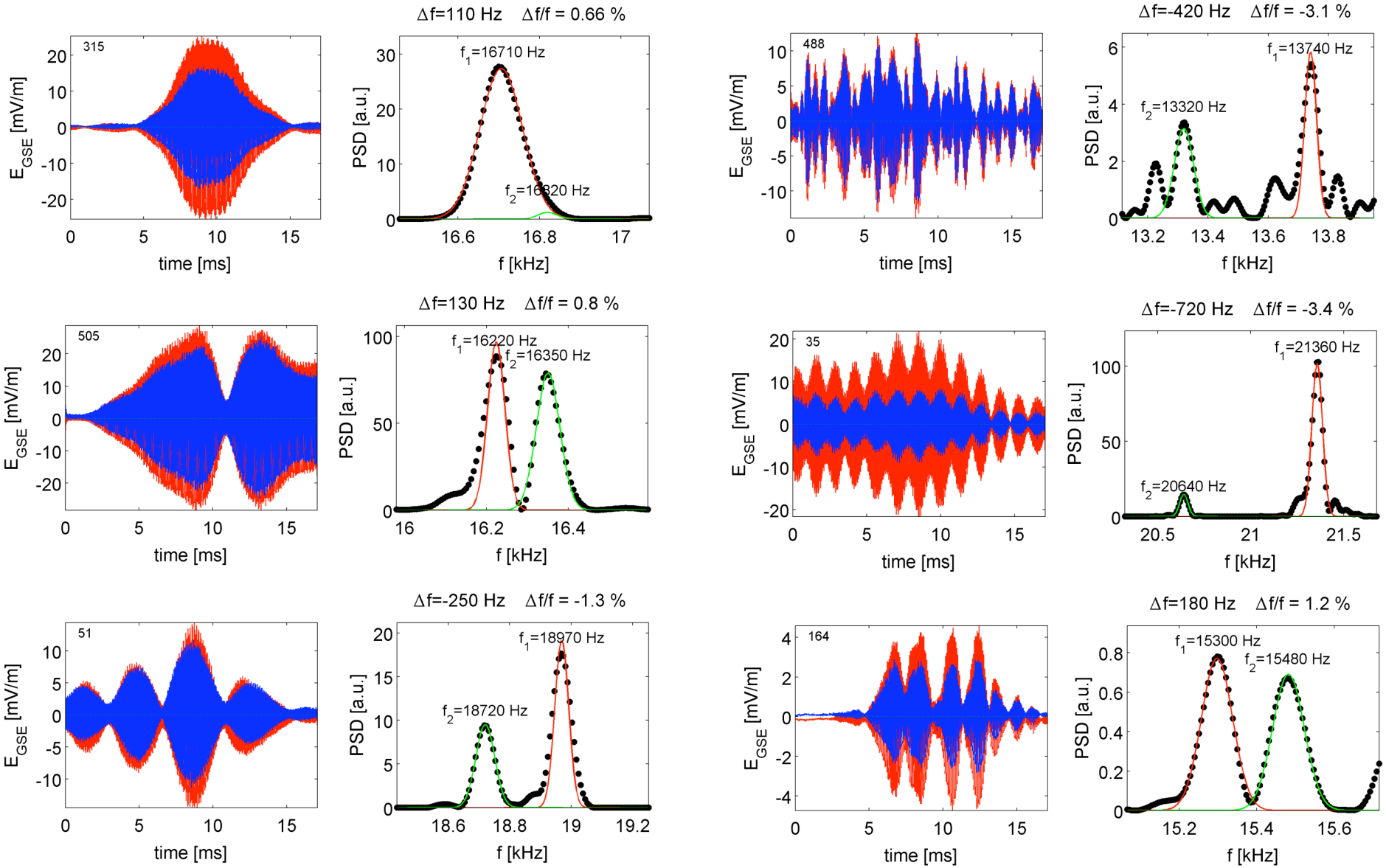

Analysis procedure

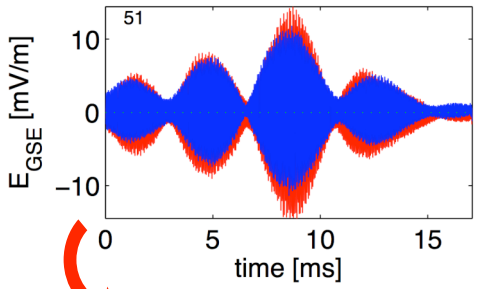

1) Initial waveforms (in GSE coordinates)

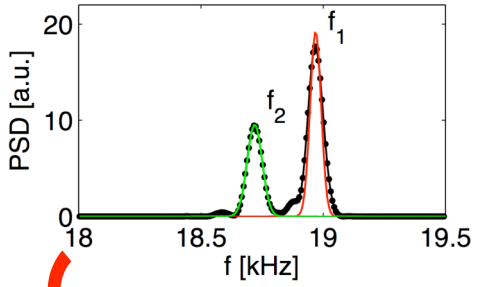

2) Compute the power spectral density
--> Locate frequencies

$$E(t) = E_1(\epsilon t)\sin\left(2\pi f_1 t + \phi_1(\epsilon t)\right) + E_2(\epsilon t)\sin\left(2\pi f_2 t + \phi_2(\epsilon t)\right)$$

3) Fit waveforms with 2 sine waves in sliding window

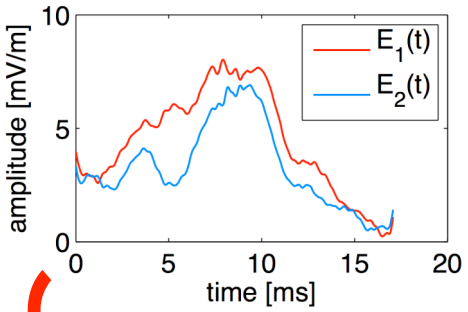

4) Check that the amplitudes vary slowly in time (no beating is allowed)

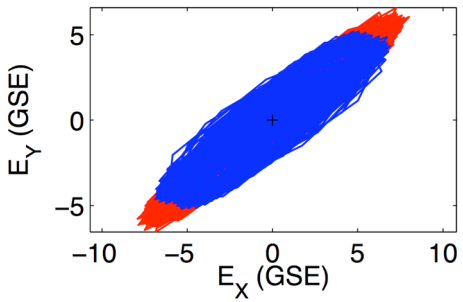

5) Plot hodograms for the two fitted sine waves

A typical hodogram

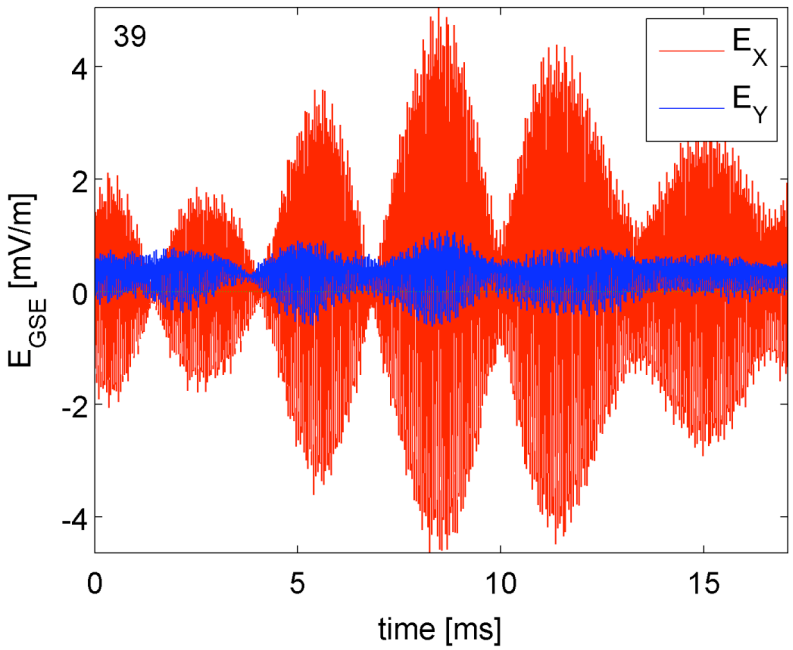

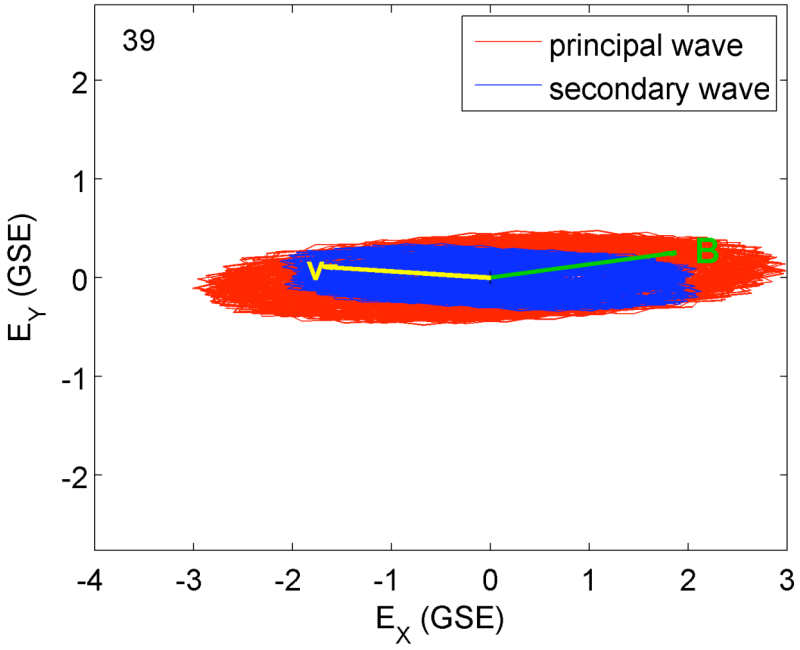

Electric field (E_X and E_Y)

Hodogram

Other hodograms

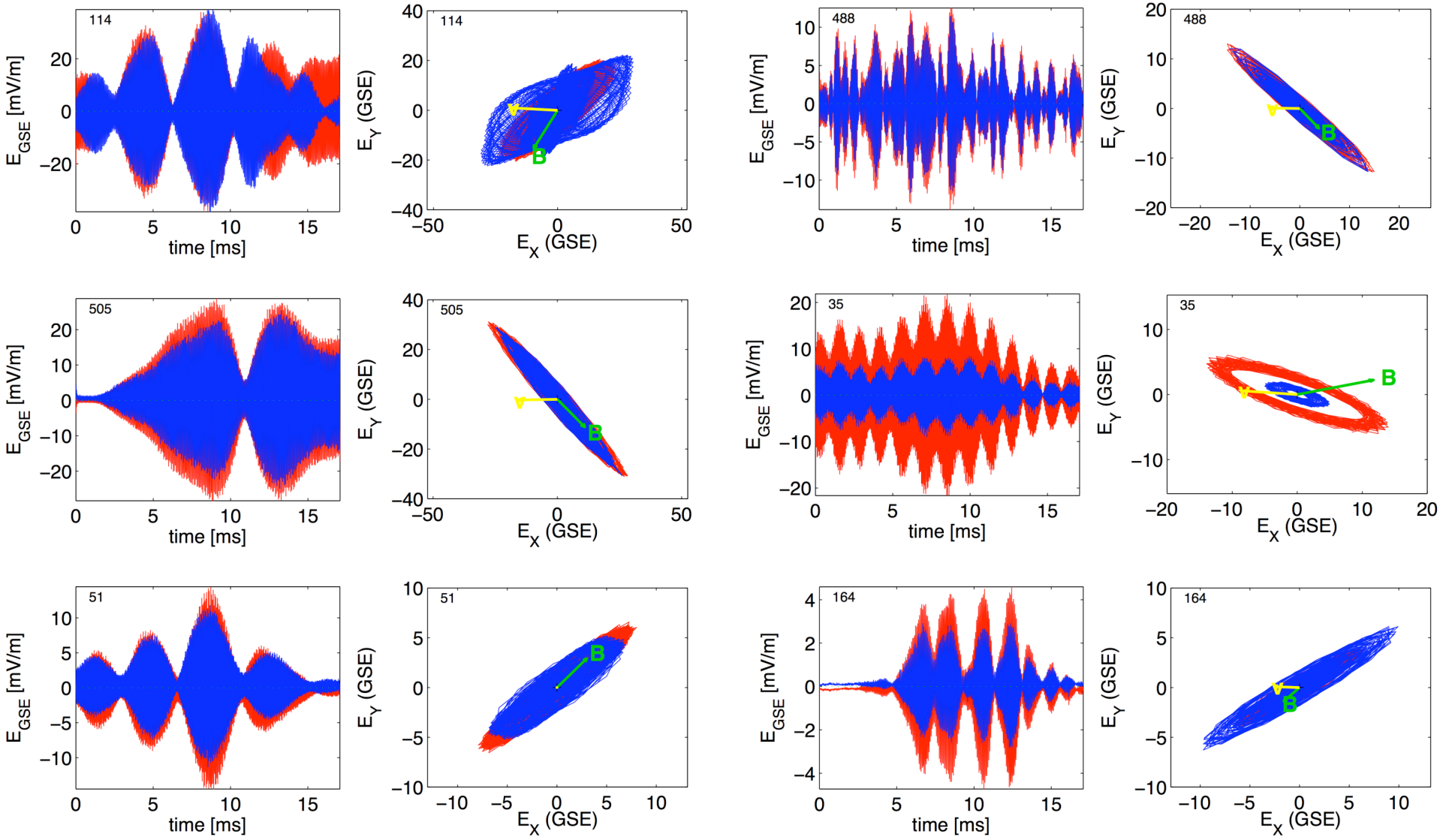

Our observations

In most cases we observe :

- A spectrum with two sharp but close spectral lines
- These frequencies are close to the plasma frequency

Case study : event #35

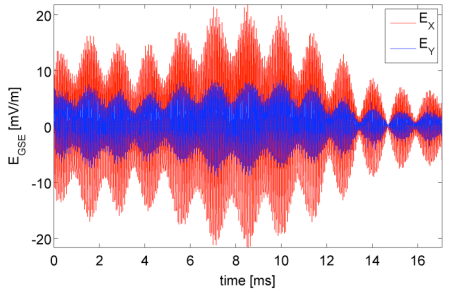

We have $f_0 = 21.36$ kHz, $f_2 = 20.64$ kHz

$$\frac{\vec{k}_0 \cdot \vec{V}_{SW}}{\omega_p} \gg \frac{3}{2} k^2 r_D^2$$

Let us assume that

$$f_0 = f_p + \frac{\vec{k}_0 \cdot \vec{V}_{SW}}{2\pi} \qquad f_1 = f_p + \frac{\vec{k}_1 \cdot \vec{V}_{SW}}{2\pi}$$

Then

$$\vec{k}_1 \approx -\vec{k}_0$$

As a firs $f_p = \frac{f_1 + f_2}{2} \approx 21$ kHz $\qquad r_D \approx 12.7$ m

Case study : event #35

Our initial hypotheses (dominant effect of Dopple shift) are well satisfied since

$$\frac{\vec{k}_0 \cdot \vec{V}_{SW}}{\omega_p} = 0.017 \gg \frac{3}{2} k^2 r_D^2 = 0.0035$$

$$\lambda = \frac{2\pi}{k_0} = \mathbf{1.42\ km}$$

This then gives

Other cases

Similar conclusions hold for

- Case #37 :

$$\begin{aligned} \lambda &= 2.31 \text{ km} \\ f_p &= 20.60 \text{ kHz} \\ kr_D &= 0.035 \end{aligned}$$

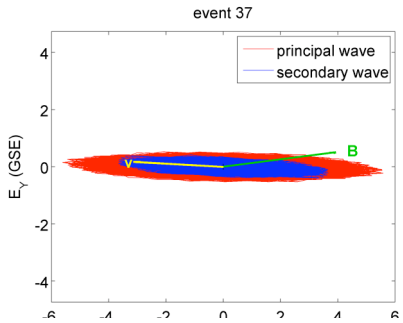

- Case #39 :

$$\begin{aligned} \lambda &= 2.57 \text{ km} \\ f_p &= 20.80 \text{ kHz} \\ kr_D &= 0.031 \end{aligned}$$

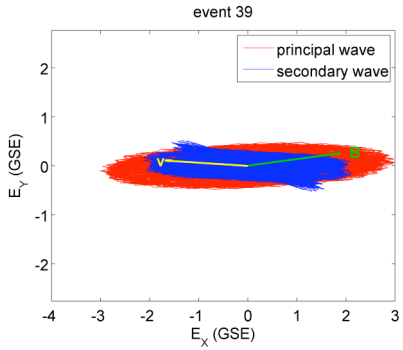

Particle distributions

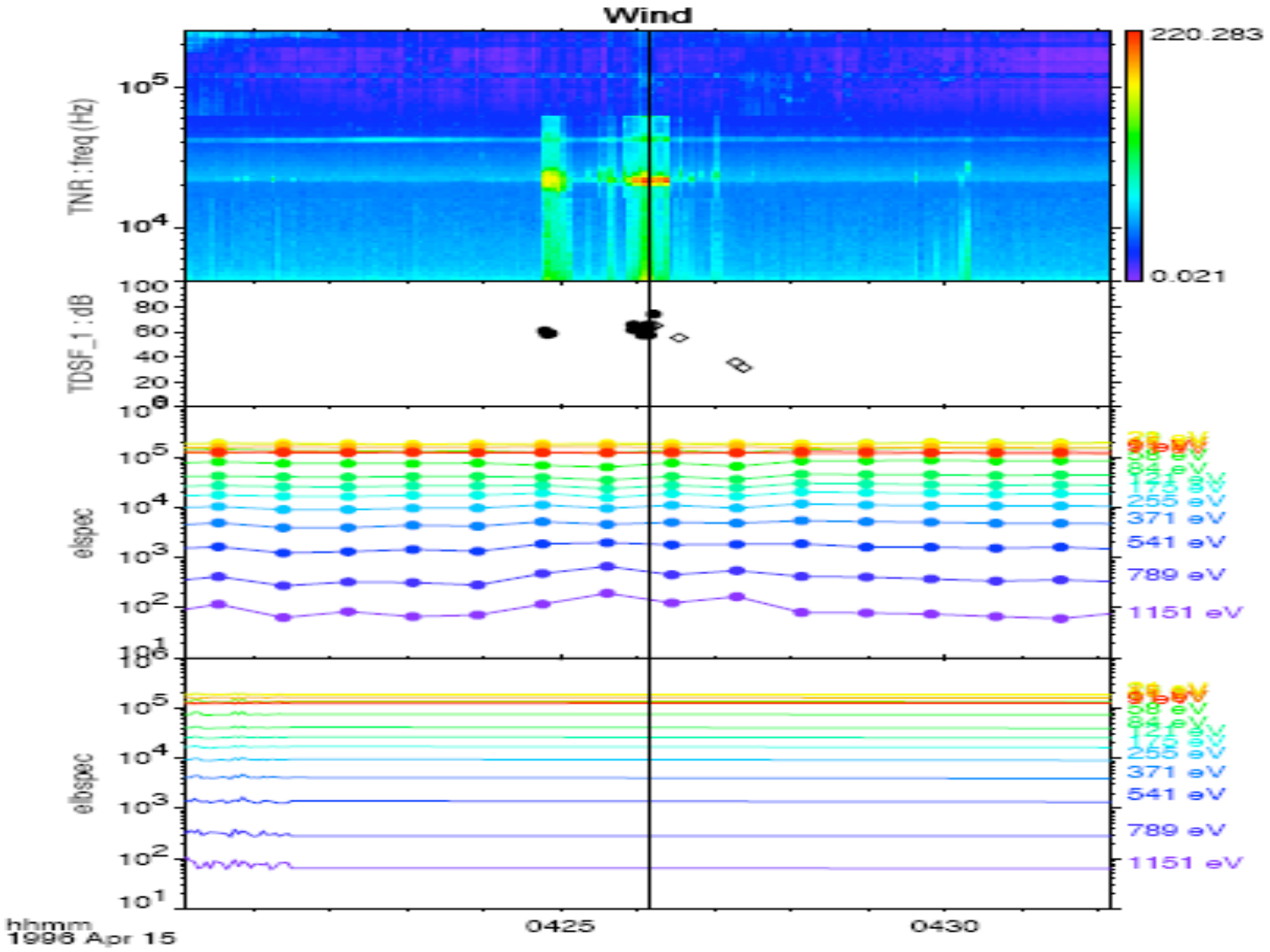

Particle distributions

- Characteristic particle energies 1 keV
- Characteristic wavelength:

Why such a difference ?

Propagation effect in nonhomogeneous plasma

Interpretation

$$E(\vec{r},t) = E_0\sqrt{\frac{k_0}{k}}\exp(i\int \vec{k}(\vec{r})\cdot d\vec{r} - i\omega t + \int \gamma(t)dt)$$

WKB wave propagation, even for γ = 0

$$E \approx \frac{1}{\sqrt{k}}$$

energy flux constant

$\Delta n / n \sim 10^{-3}$

Propagation to denser plasma results in decreasing of k – vector and of wave damping on thermal electrons for HF and LF waves

Conclusions (1/2)

- Our analysis of polarization properties of waves observed in the boundary between the solar wind and electron foreshock region by the WIND satellite shows that some of these waves are Langmuir waves.
- Their spectra consists of two clearly identifiable peaks separated in frequency.
- These spectral properties can be

Conclusions (2/2)

When the solar wind speed is large enough and is directed closely to the magnetic field, the wave vectors of primary and secondary waves are almost collinear and their direction is close to the direction of the background magnetic field.

- Using the directivity of the k-vectors we can evaluate the **wavelength** of the waves and the **characteristic lengths** of the wave packets.

Problem to solve

- Electrostatic Langmuir wave propagates towards the point of reflection and in unperturbed plasma the reflected Langmuir wave is strongly damped
- Evaluate the increment of the absolute decay instability and characteristic frequency and k-vector of the generated secondary Langmuir wave and ion-sound wave

Problem II to solve

- The beam propagates in a weakly magnetized plasma with density fluctuations described by the probability distribution P(a, δN), a –characteristic scale, δN – density fluctuations aplitude, that can be chosen for convenience
- Determine the average characteristics of plasma waves and the length of the relaxation of the beam

Two remarks

- http://stamms2.cnrs-orleans.fr/
- http://www.copernicus.org/EGU/annales/published_papers.html